European Commission

JRC TECHNICAL REPORTS

Physicochemical characterisation of gold, silica and silver nanoparticles in water and in serum-containing cell culture media

Drewes C.C., Ojea Jimenez I., Mehn D., Colpo P., Gioria S., Bogni A., Ponti J., Kinsner-Ovaskainen A., Gilliland D., Riego Sintes J.

2018

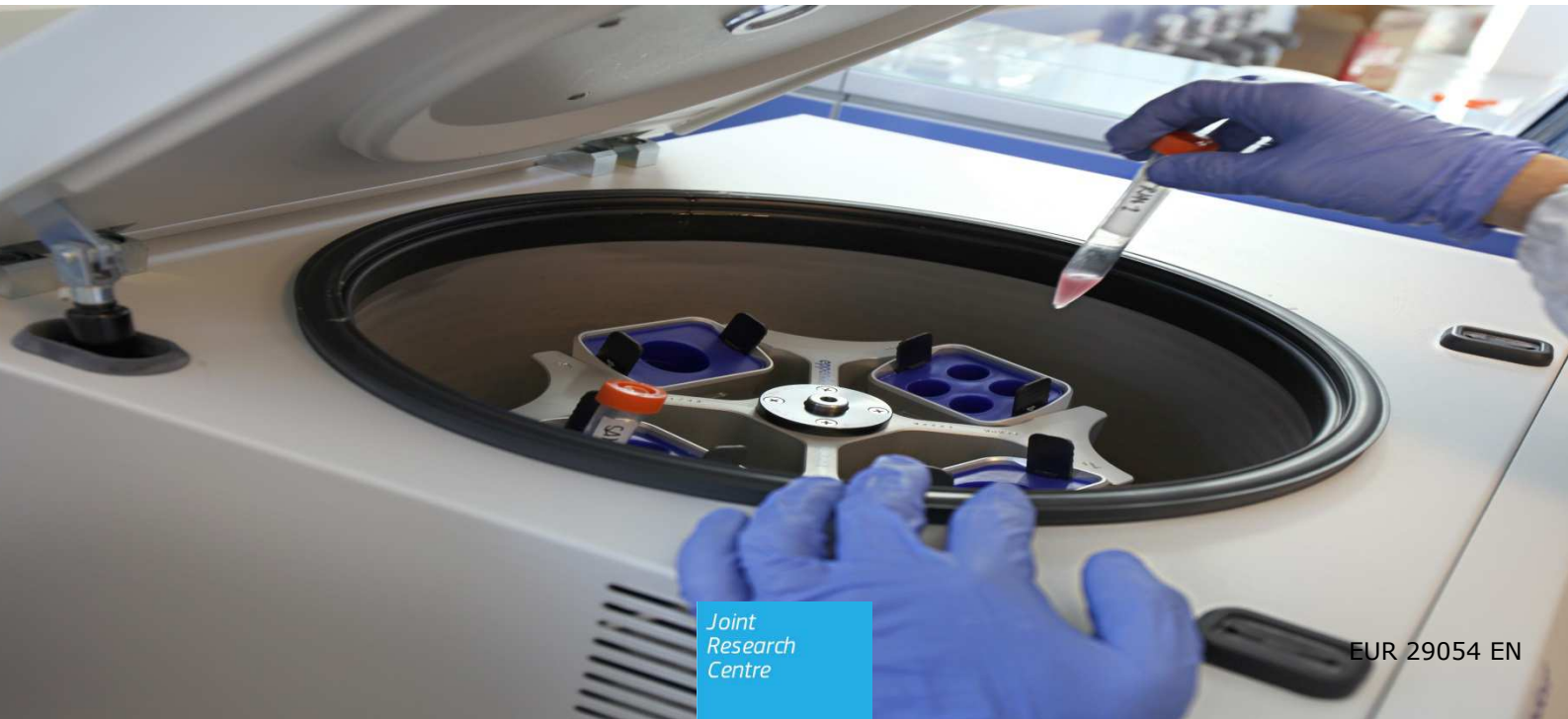

Joint Research Centre

EUR 29054 EN

Contact information
Name: Pascal Colpo
Address: TP 125
Email: JRC-NANOTECHNOLOGY@ec.europa.eu
Tel.:

JRC Science Hub
https://ec.europa.eu/jrc

JRC110379

EUR 29054 EN

PDF	ISBN 978-92-79-77705-9	ISSN 1831-9424	doi:10.2760/818663
Print	ISBN 978-92-79-77704-2	ISSN 1018-5593	doi:10.2760/58721

Luxembourg: Publications Office of the European Union, 2018

How to cite this report*: Drewes C.C* et al, *Physicochemical characterisation of gold, silica and silver nanoparticles in water and in serum-containing cell culture media*, EUR 29054 EN, Publications Office of the European Union, Luxembourg, 2018, ISBN 978-92-79-77705-9, doi 10.2760/818663, PUBSY No. JRC110379

Contents

Foreword

The European Commission's Joint Research Centre (JRC) provides scientific support to European Union policies, including nanotechnology. The increasing use of manufactured nanomaterials (NMs) in a number of commercial applications and consumer products raises questions regarding potential unintended risks to humans and the environment. For a number of years the JRC has been active in the development, optimisation and harmonisation of test methods suitable for hazard assessment of NMs. International harmonisation of these test methodologies is ensured, among others, through JRC's participation in the Organisation for Economic Co-operation and Development (OECD) Working Party of Manufactured Nanoparticles (WPMN).

The OECD WPMN's programme on the safety of manufactured nanomaterials addresses all the different components needed for thorough risk assessments for human health and the environment, including the availability of reliable methods for the purpose of NMs safety assessment. At an expert meeting held in Paris in October 2014 it was concluded that the scientific information available to date is not sufficient to fully support a harmonised version of the *in vitro* micronucleus test protocol because the existing or published data were not generated in a harmonised way and do not provide answers to some key questions. In particular, questions remain regarding the uptake on NMs, dosing regimens, necessary length of exposure to NMs or scheme of treatment to cytochalasin B. The OECD WPMN approved a JRC led project aiming at the adaptation of the *in vitro* micronucleus test (Test Guideline 487) for the assessment of manufactured NMs that was subsequently included by the OECD-WNT in the work plan of the Test Guidelines Programme (Project 4.95). Therefore, work aiming to develop a Guidance Document (GD) addressing the necessary adaptations of current genotoxicity TGs for nanomaterials testing was initiated under the coordination of JRC. This report summarises the results of the first stage of the project.

Acknowledgements

Carine Cristiane Drewes wishes to thank the Brazilian National Council of Technological and Scientific Development (CNPq, Brazil, Process number 200259/2015-6) for the support received.

Authors

Carine Cristiane Drewes

Isaac Ojea Jimenez

Dora Mehn

Pascal Colpo

Sabrina Gioria

Alessia Bogni

Jessica Ponti

Agnieszka Kinsner-Ovaskainen

Douglas Gilliland

Juan Riego Sintes

Abstract

This report presents the results from a study organised under the coordination of JRC as part of a project aiming at the adaptation of the *in vitro* micronucleus test (Test Guideline 487) for the assessment of manufactured NMs. The aim of the first step of the project was to evaluate the physicochemical characterisation of selected representative nanomaterials (5 nm gold, 30 nm gold, 22 nm silica, 30 nm citrate and 30 nm PVP stabilised silver nanoparticles) in pure water and in different complete culture media.

The results of the study show that using a combination of different characterisation techniques is important to providing reliable information about the agglomeration[1] behaviour of the tested nanoparticles in complete cell culture media (CCM). Most of the materials exhibited mild agglomeration in serum containing CCM. Only the PVP functionalised silver nanoparticles showed a size distribution change in all of the culture media that is so small that it could be attributed to solely protein adsorption without notable agglomeration. Silica nanoparticles were found to be the most sensitive to interaction with serum containing CCM, showing massive concentration and time dependent agglomeration strongly affected by the CCM composition. Extensive agglomeration might lead also to the accelerated sedimentation of the particles changing drastically the true, effective dose that the cells will receive under *in vitro* conditions[1] . Thus, it has to be investigated in more detail and taken in account when designing *in vitro* experiments in the next phase of the project.

[1] See section on abbreviations nomenclature

1 Introduction

A "Nanomaterial" according to the European Commission recommended definition is a natural, incidental or manufactured material containing particles, in an unbound state or as an aggregate or as an agglomerate and where, for 50 % or more of the particles in the number size distribution, one or more external dimensions is in the size range 1 nm - 100 nm. [3] Nanomaterials are used in a variety of industrial sectors and in numerous consumer products, such as paint, catalysts, sports items, surface treatment products, textiles, cosmetic products, food additives and packaging, vehicle tyres, electronic items and analytical chemical equipment. Some applications are new, while others, such as paint and catalysts, have been around for many years.

Nanomaterials (NMs) are often well-known chemical substances that can exhibit new physical and chemical characteristics when produced in a nanoform. Gold for example, in bulk form, is typically an inert, shiny yellow metal but in nanoform can become very catalytically active or show optical properties which change depending on particle size and shape. Other examples of new characteristics that materials may possess at the nanoscale are anomalous electrical conductivity and superparamagnetism. The complexity of nanomaterial behaviour stems from the fact that the same chemical substance can be used in a variety of different nanoforms that may display a wide range of properties including size, shape, surface functionalisation, surface charge, that affect their way of interacting with biological systems such as biological fluids (protein-surface interactions) and living cells (cellular uptake, mechanisms of toxic response). This renders their safety assessment challenging.[4-7]

Nanotechnology is a rapidly developing field and it is expected that an increasing number of new NMs will be developed and put on the market in the near future. To enable a quick and reliable safety assessment of NMs used in consumer products, there is an urgent need to provide robust, standardized *in vitro* test methods for toxicity screening. However, due to the special properties of these materials (including their high surface area) they may show unexpected interferences in classical *in vitro* toxicity assays.[8-14]

The EC JRC is contributing to the development and optimisation of *in vitro* methods suitable for the hazard assessment of NMs.[6, 11, 15] Well-established *in vitro* methods for the testing of chemicals are adapted for NMs by investigating possible interferences of the NMs with the assays. The JRC study presented here is focused on the relationship between the physicochemical properties of the NMs under *in vitro* conditions and the observed biological response. Special attention is paid to the development of methods for NM dosimetry to quantify the effective cellular dose. This work is performed in collaboration with the OECD Working Party on Nanomaterials (WPMN).[16-18]

The first phase of the study includes the identification of the necessary changes in the protocol of the micronucleus *in vitro* assay (TG487) when used to test NMs, taking into account the physicochemical characterisation of NMs, kinetics of intracellular uptake and NMs dosimetry *in vitro*. This report presents the results and conclusions from the physicochemical characterisation of selected nanoparticles for Adaptation of *In vitro* Mammalian Micronucleus Test Guideline (TG 487) for Testing of Manufactured Nanomaterials.

2 Synthesis, sourcing and physicochemical characterisation of stock suspensions

2.1 Materials

The nanoparticles (NPs) used in this study were obtained either by in-house synthesis (AuNPs of 5 and 30 nm diameter and SiO_2NPs of 22 nm diameter) or from the supplier nanoComposix (30 nm Cit-AgNPs and PVP-AgNPs). Table 2.1 summarises the representative nanoparticles (NPs) selected for the study.

Table 2.1 List of nanomaterials tested in the study

NPs name	Nominal size (nm)	Batch number	Supplier
AuNPs	5	IO176A	JRC in-house synthesis
AuNPs	30	IO194B	JRC in-house synthesis
Cit-AgNPs	30	DMW0208	NanoComposix
PVP-AgNPs	30	MXR0002	NanoComposix
SiO_2NPs	22	IO122B	JRC in-house synthesis

In case of the in-house synthesised materials the following sections will detail the synthesis method and principal physicochemical characteristics of the materials as determined shortly after synthesis. The Cit-AgNPs and PVP-AgNPs which were purchased from the commercial supplier NanoComposix were initially in suspension and the synthesis routes will not be detailed but physicochemical properties will be reported.

The cell culture media (CCM) tested in the study in the presence of serum together with their commercial source information are summarised in Table 2.2. All complete culture media contained Penicillin – Streptomycin at 100 x dilution (at concentrations of 100 U/mL and 100 µg/mL).

Table 2.2 List of serum-containing cell culture tested in the study

Short Name	Culture Media	Serum
F12+10CS	F12 (Ham's F12, Gibco®)	10% Calf Serum (Gibco®)
DMEM+10FBS	DMEM (Dulbecco's Modified Eagle Medium, Gibco®)	10% Foetal Bovine Serum (Gibco®)
MEM+20FBS	MEM (Minimum Essential Medium, Gibco®)	20% Foetal Bovine Serum (Gibco®)
RPMI+10HS	RPMI 1640 (Roswell Park Memorial Institute, Gibco®)	10% Horse Serum (Gibco®)

All other chemicals were purchased from Sigma Aldrich and used without further modifications.

2.2 Characterisation methods

Stock suspensions of each NP sample were characterised using various techniques such as UV-Visible spectroscopy (UV-vis), Dynamic Light Scattering (DLS), Centrifugal liquid sedimentation method (CLS), Transmission Electron Microscopy (TEM).

2.2.1 UV-Visible spectroscopy

Metallic NPs with sizes smaller than the wavelength of light show strong dipolar excitations in the form of localized surface plasmon resonances. The resonance frequency of the oscillation, i.e. the plasmonic peak position of these materials depends on the dielectric properties of the metal and the surrounding medium and on the size and shape of the metallic particles. A shift in the λ_{max} value of a metallic NP suspension to higher wavelengths might indicate the presence of an adsorbed layer on the particles and/or particle aggregation/agglomeration.[19, 20]

UV-Vis spectra of stock solutions of gold and silver NPs were recorded with an Evolution 300 UV-Vis Spectrophotometer (Thermo Scientific, USA) at room temperature.

2.2.2 Dynamic light scattering

DLS provides information about the hydrodynamic diameter distribution of the NPs in suspension. The resulting values are generally higher than particle sizes detected by electron microscopy because of the presence of hydration layer, protein corona or functionalisation and because results are generally biased in the presence of a small fraction of large particles or agglomerates*. This latter effect derives from the fact that (in a certain particle size range) the intensity of the scattered light is proportional to the sixth power of the radius of the nanoparticles. As a result, a small fraction of large particles may produce a strong optical signal which completely masks a large fraction of smaller particles. DLS does not distinguish between constituent particles and aggregates/agglomerates. It simply gives information about all diffusing ensembles, regardless of whether they are individual particles, agglomerates or aggregates. Consequently, DLS analysis of a polydisperse NP mixture will usually produce results which tend to reflect the size of the larger particles present in a solution even when these numerically constitute only a minor fraction of the total population.[21, 22]

Particle size distribution (PSD) was determined by Dynamic Light Scattering (DLS) using a Zetasizer Nano-ZS instrument (Malvern Instruments Ltd, UK) with temperature control (25°C). Each sample was recorded in quadruplicate with an equilibration step of 120 sec. The instrument was set to automatic acquisition mode. Hydrodynamic diameters were calculated from the intensity-weighted particle size distributions derived from the measured correlogram using a NNLS fitting algorithm.

2.2.3 Centrifugal liquid sedimentation

Particle size measurement by Centrifugal Liquid Sedimentation (CLS) operates on the principle of separating particles by size and density using centrifugal sedimentation in a liquid medium. In the version of this technique more correctly known as "Line-start CLS" particles are injected into a liquid medium contained within an optically clear, rotating disc. Once the particles enter the rotating liquid media they sediment radially outwards at speed which is a function of their density and Stokes diameter. At a certain point in time the particles pass through a narrow beam of light which shines through a region near the outside edge of the rotating disc. As the particles pass through the detector beam the light is partially scattered and the transmitted light intensity decreases as function of concentration and size of the particles. Simultaneously, the particle size is calculated from the sedimentation time. To establish the relationship between sedimentation time and particle size, each analysis is preceded by a calibration run performed using a narrowly distributed size standard. In order to stabilize sedimentation and avoid streaming, the spin fluid should have a small density gradient. During each measurement run the variation in light intensity is continuously recorded as a function of

sedimentation time and converted into an extinction-based size distribution that can be further transformed to a mass or number based distribution applying the Mie theory and using absorption, refractive index, and particle density as input parameters, and assuming the particles have a spherical shape. It should be noted that by using an operator input value for particles density, the Stokes diameters derived from CLS measurements might be biased if the real density of the sedimenting particles differs significantly from the expected (bulk) density of the material. This can typically occur with small NPs in the presence of an adsorbed layer (protein corona, functionalisation, etc.) with much lower density than the core material.[2, 23]

In order to assess the particle size distributions of the nanoparticles, CLS characterisation was performed on the as synthesized nanoparticle dispersions. Measurements were run using a disc centrifuge (model DC24000UHR CPS Instruments), in an 8 wt% - 24 wt% sucrose density gradient at a disc rotational speed of 22000 rpm. Each sample injection of 100 µL was preceded by a calibration step performed using certified poly(vinyl chloride) (PVC) particle size standard with mean diameter of 239 nm (CPS Instruments).

2.2.4 Transmission electron microscopy

Transmission electron microscopy (TEM) allows direct imaging of the NPs. Combined with statistical analysis of the micrographs (with the help of image analysis software), TEM provides information on particle shape and number based size distributions. However, for good quality image analysis, the particles should be well dispersed and distributed on the grid. Unfortunately, simple TEM sample preparation methods (i.e. evaporation of the solvent) do not distinguish between agglomerates formed during the drying of the sample drop on the support (grid) and aggregates that were already present in the NP suspension.

TEM analysis was done following the spotting of liquid particle dispersions on copper support grids. A drop of undiluted product (4 µL) was placed onto ultrathin Formvar-coated 200-mesh copper grids (Tedpella Inc.) and left to dry in air at 4°C. NPs were visualized using TEM (JEOL 2100, Japan) at an accelerating voltage of 200 kV. Digital micrographs were analysed using the ImageJ software and a custom macro performing smoothing (3x3 or 5x5 median filter), manual global threshold and automatic particle analysis provided by ImageJ. For each sample, the size of at least 60 particles was measured to obtain an average diameter and the size distribution.

2.2.5 Inductively Coupled Plasma Mass Spectrometry

Inductively Coupled Plasma Mass Spectrometry (ICP-MS) provides quantitative information about the elemental composition of the samples. ICP-MS measurements were performed using an Agilent 7700 ICP-MS instrument (Agilent Technologies Inc., USA) after acid digestion of the samples.

2.3 Gold nanoparticles

2.3.1 In house synthesis of gold nanoparticles

The synthesis of the sodium citrate-stabilised 5 nm gold nanoparticles (Au NPs) was carried out by reduction of gold (III) chloride hydrate salt with the strong reducing agent NaBH4. Briefly, 96 mL of a sodium citrate solution (0.25 mM) in MilliQ water was stirred in an ice bath, to which 1 mL of aqueous solution of gold (III) chloride trihydrate (25 mM) was added. Then, 3 mL aqueous solution of sodium borohydrate (100 mM) was quickly added to the gold salt solution under vigorous stirring. The reduction of gold salt to gold nanoparticles by the sodium borohydrate produced a change in colour of the liquid from pale yellow to dark red. The suspension was then stirred in the ice bath for further 30 min and then left to warm to room temperature. The final pH value of the solution was 6.7 and the estimated nominal Au concentration (stoichiometry) was 0.25 mM.

For the physico-chemical characterisation in different cell culture media (CCM), AuNPs 5 nm were concentrated by centrifugal ultrafiltration using AMICON ULTRA-15 10 KDa filter tubes (Millipore, Milan, Italy). 10 mL AuNPs suspension was placed in each filter tube and centrifuged at 1500 rcf at room temperature for 20 min during which time the sample volume was reduced from 20 mL to 1.2 mL. The final concentration of the stock suspension measured by ICP-MS resulted to be 5.05 mM. The stock suspension was stored at 4°C in dark.

The in-house synthesis of 30 nm AuNPs was carried out by a two-step seed growth method in which the reduction of gold (III) chloride hydrate salt in the presence of trisodium citrate dihydrate was used to selectively enlarge highly mono-dispersed 12 nm size gold seed particles. In the first step of the process, the 12 nm seed particles were obtained by a method adapted from that described by Turkevich et al.[24] Briefly, the solution was heated up using a microwave apparatus (Discover S by CEM corporation) to ensure a highly reproducible rapid heating. In this method, 5 mL of tetrachloroauric acid trihydrate ($HAuCl_4$ x $3H_2O$, 10 mM) was dissolved in 95 mL of water. The solution was rapidly heated up and held at 97°C for 5 min using a microwave power of 250 W under vigorous mechanical stirring; 2.5 mL of trisodium citrate dihydrate (100 mM) was added to the solution and kept at 97 °C for another 20 min. Afterwards, the solution was rapidly cooled down to 40°C and then to room temperature. The gold nanoparticles were produced by the reduction of the gold salt by sodium citrate that acted as both reducing agent and stabiliser. The final suspension contained 12 nm size gold nanoparticles (0.5 mM gold concentration) stabilized with 2.5 mM of sodium citrate at pH 6-7.

In the second stage of the synthesis, 95 mL of MilliQ water was left to stir at 60°C for two hours. Sequentially, 2.8 mL of sodium citrate dehydrated (100 mM) and 0.420 mL of sodium hydroxide (200 mM) were added to the water and left to equilibrate for 30 min. Then 2.24 mL of tetrachloroauric acid trihydrate 10 mM ($HAuCl_4$ x $3H_2O$) and 0.6 mL of the 12 nm gold nanoparticles with a gold concentration of 0.5 mM were added to the solution, under vigorous stirring. The solution was left to react for 48 h at 60°C. The final suspension contained 30 nm AuNPs stabilised with 2.8 mM of sodium citrate at pH 6.7. The calculated nominal gold concentration was 0.225 mM.

For the physicochemical characterisation in different CCM, 30 nm AuNPs were concentrated by centrifugal ultrafiltration using the AMICON 10 KDa filter tubes (Millipore, Milan, Italy); 10 mL AuNP suspension was added on each filter and tubes were centrifuged for 20 min at 1500 rcf at room temperature. The final gold concentration was measured by UV-Vis and found to be 5.89 mM. This stock suspension was stored at 4°C away from light.

2.3.2 TEM, UV-Visible, DLS and CLS characterisation of gold nanoparticles

TEM micrographs of the 5 nm and 30 nm AuNPs are shown in Figure 2.1 together with results of the size distribution analysis. As a result of the sample preparation procedure (dried drop), particles appear as agglomerates in the TEM micrographs. Statistical size analysis after fitting the size distributions with a Gaussian distribution provided mean diameter values of 4.8 nm and 32 nm for the 5 and 30 nm nominal diameter particles, respectively.

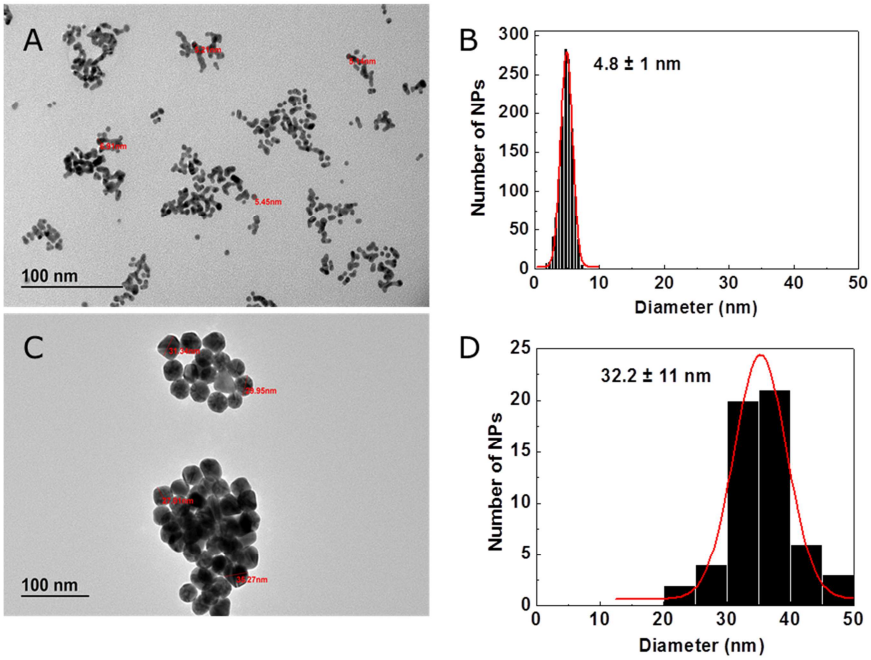

Figure 2.1 TEM micrographs and number based particle size distributions with Gaussian fit of (A,B) and 5 nm AuNPs (C,D).

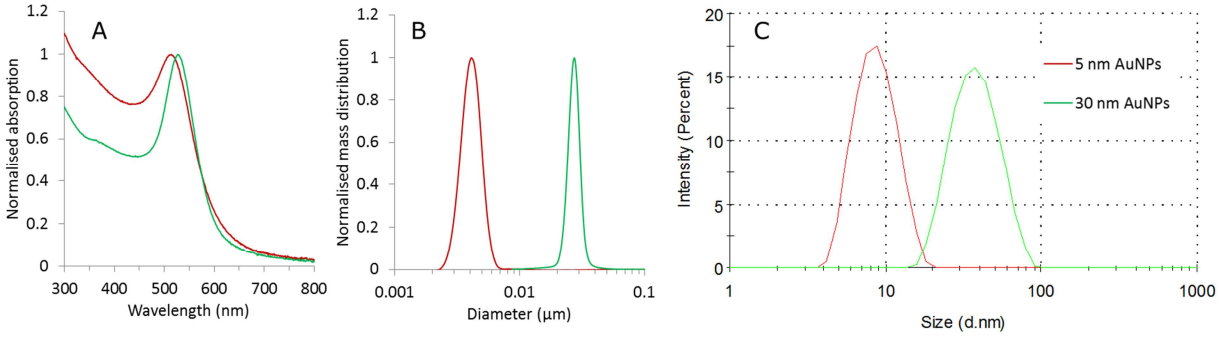

Figure 2.2 UV-Vis spectra (A), CLS mass based size distributions (B) and DLS intensity based size distributions (C) of 5 nm (red) and 30 nm (green) gold nanoparticles.

UV-Vis spectra (Figure 2.2 A) of the AuNPs show one well defined plasmonic peak (at 514 nm and 527 nm), for each material at the expected wavelength corresponding to their diameters.[25]

CLS measurements (Figure 2.2 B) suggested 4 nm and 27 nm size (mass based size distribution mode) for the two different AuNP suspensions. These values are very close to the TEM results (Table 2.3). The apparent shift to slightly lower diameters might be because of the effect of the hydration layer on the particle densities that causes longer sedimentation times than theoretically expected.[23]

Hydrodynamic diameters (Figure 2.2 C) determined from the intensity based distribution means (9 and 39 nm) are higher than the TEM and CPS sizes due to the hydration layer covering the particles in aqueous suspension, or due to the width of the size distribution, or to a combination of both. All measurements suggest that the stock suspensions are monomodal, containing particles close to the expected nominal dimensions.

2.4 Silica nanoparticles

2.4.1 In house synthesis of silica nanoparticles

The 22 nm SiO_2NPs were synthesised using a method adapted from Hartlen et al.[26]. Briefly, cyclohexane (16.25 mL) was mixed with a solution of L-arginine (330 mg, 1.9 mmol) in MilliQ water (250 mL). The mixture was heated to 50°C at a constant stirring rate of approximately 300 rpm before TEOS (20 mL) was slowly added and the reaction was kept under these conditions for 24 h.

The concentration of 22 nm SiO_2NPs in the stock suspension measured by gravimetric technique was 2.2 mg/mL. The stock suspension was stored at 4°C in dark.

For the physicochemical characterisation in different CCM, 22 nm SiO_2NPs were concentrated by centrifugal ultrafiltration using the AMICON 10 KDa filter tubes (Millipore, Milan, Italy); 10 mL SiO_2NP suspension was measured in each filter tube and centrifuged for 20 min at 1500 rcf at room temperature. The final concentration was measured by gravimetric technique and found to be 8.8 mg/mL. The stock suspension was stored at 4°C away from light.

2.4.2 TEM, DLS and CLS characterisation of silica NPs

TEM micrographs of the 22 nm SiO_2NPs (Figure 2.3 A) show particles with an equiaxial shape. Statistical size analysis after fitting the number based size distribution with a Gaussian fit provided a mean ECD (equivalent circle diameter) value of about 20 nm.

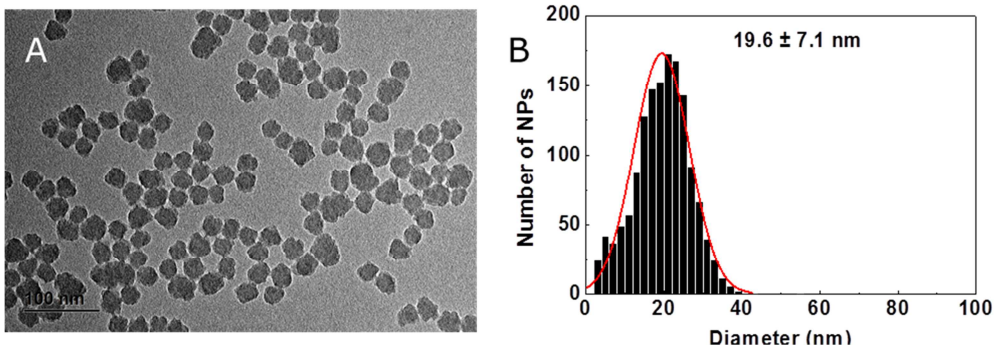

Figure 2.3 TEM micrograph (A) and number based particle size distribution with Gaussian fit of (B) 22 nm SiO2NPs.

CLS measurement (Figure 2.4 A) suggested 23 nm size (modal value of the mass based size distribution) what is very close to the TEM diameter (Table 2.3).

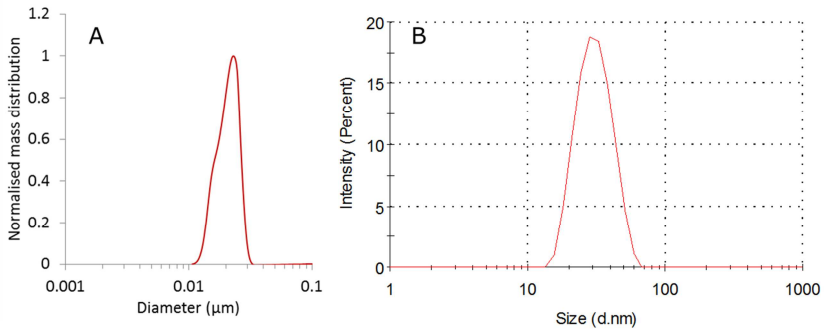

Figure 2.4 CLS mass based size distribution (A) and DLS intensity based size distribution (B) of the 22 nm silica nanoparticles.

Hydrodynamic diameter of the SiO_2-NPs (Figure 2.4 B) determined from the intensity based distribution mean (31 nm) is higher than the TEM and CPS sizes - most probably both due to the hydration layer covering the particles in aqueous suspension and due to the bias caused by larger, more scattering particles. All measurements suggest that the stock suspension is monomodal, containing particles close to the expected nominal dimension.

2.5 Silver nanoparticles

Cit-AgNPs (30 nm) and PVP-AgNPs (30 nm) were purchased from NanoComposix.

Cit-AgNPs were provided as a suspension containing 1.02 mg/mL silver (corresponding to a particle concentration of $5.3x10^{12}$ particles/mL) in an aqueous 2 mM citrate solution. They were reported to have a TEM diameter of 32.7 ± 4.8 nm, hydrodynamic diameter (DLS? Which DLS method?) of 35.6 nm, and a plasmonic peak at λ_{max}= 403 nm.

PVP-AgNPs were provided as a suspension containing 1.08 mg/mL silver (corresponding to a particle concentration of $5.6x10^{12}$ particles/mL) in MilliQ water. They were reported to have a TEM diameter of 32.7 ± 4.3 nm, hydrodynamic diameter of 51 nm, and a plasmonic peak at λ_{max}= 403 nm.

2.5.1 TEM, UV-Vis, DLS and CPS characterisation of silver nanoparticles

In house TEM analysis of the Ag-NPs confirmed the spherical shape and the expected size of the particles.

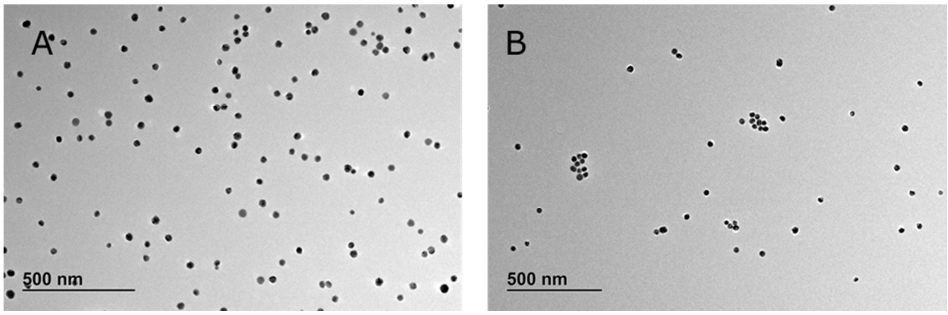

Figure 2.5 TEM micrographs of the 30 nm Cit-AgNPs (A) and 30 nm PVP-AgNPs (B).

UV-Vis spectra of the Cit-AgNPs and PVP-AgNPs (Figure 2.6 A) were perfectly overlapping with negligible difference in the absorption peak maximum position (401 nm and 399 nm, respectively). The UV-Vis results also confirm, that the two silver particle samples have very similar sized metallic core.

CLS measurements suggested apparently lower Stokes diameter for PVP-AgNPs than for Cit-AgNPs (Figure 2.6 B, Table 2.3). This apparent decrease in the particle size can be explained by the presence of the PVP coating on the particles, which leads to decreased total particle density and - as a consequence – longer sedimentation times. In standard computations using bulk silver density (10.49 g/mL) the longer sedimentation times will (incorrectly) result in lower calculated particle diameters.

Considering the presence of the PVP coating, it is not surprising that DLS hydrodynamic diameter of the PVP-AgNPs was higher than the diameter of Cit-AgNPs (Figure 2.6 C) with higher polidispersity index (Table 2.3). However, all characterisation techniques suggest that the stock suspensions are monomodal, containing particles close to the declared nominal dimension.

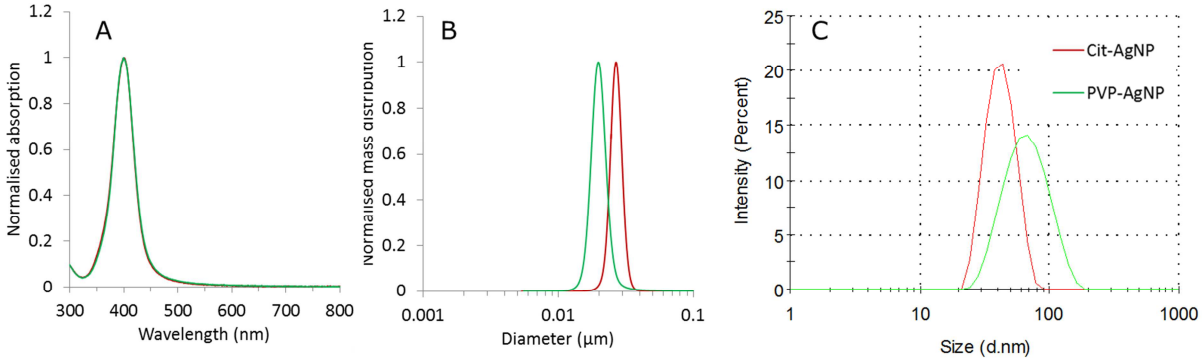

Figure 2.6 UV-Vis spectra (A), CLS mass based size distributions (B) and DLS intensity based size distributions of 30 nm (C) Cit-AgNPs (red) and PVP-AgNps (green).

2.6 Summary of morphology and sizing of all stock solutions

TEM analysis was performed to determine the shape of the particles and to verify whether the PSD results from DLS and CLS measurements were representative of the single particles or agglomerates. The DLS and CLS measurements were conducted as described above on stock dispersions of the NPs (diluted in MilliQ water if necessary) and the results obtained are summarised in Table 2.3. The morphology of all NPs stock solutions obtained by transmission electron microscopy analysis is presented in Figure 2.7.

Table 2.3 Characterisation of size distribution (by TEM, DLS and CLS) of the stock suspensions NPs. TEM: number based mean diameter. DLS: Intensity based mean diameter. CLS: mass based size distribution mode.

NPs	Nominal size (nm)	Size distribution		
		TEM (nm ± SD)	DLS (nm /PdI[1])	CLS (nm/HHW[2]/PdI[3])
AuNPs	5	4.8 ± 1.0	9/0.21	4/2/1.6
AuNPs	30	32 ± 11	39/0.25	27/7/1.2
SiO_2NPs	22	20 ± 7	31.4/0.06	23/11/1.1
Cit-AgNPs	30	33 ± 5*	43.1/0.06	27/6/1.1
PVP-AgNPs	30	33 ± 4*	70.5/0.17	20/6/1.1

[1]DLS Polydispersity Index
[2]Full Width at Half Maximum (FWHM)
[3]CLS Polydispersivity Index (Dw/Dn) defined as distribution width of NPs' mass based size distribution divided by distribution width of the NPs' number based size distribution.
* Data provided by supplier

TEM images show that all the particles can be considered to be equiaxial and often approximately spherical and thus the generally used models are suitable in DLS and CLS based size estimations. A comparison of the TEM determined sizes with the hydrodynamic diameters (DLS size measures) show that hydrodynamic diameter values are generally higher than expected from TEM and CLS data.

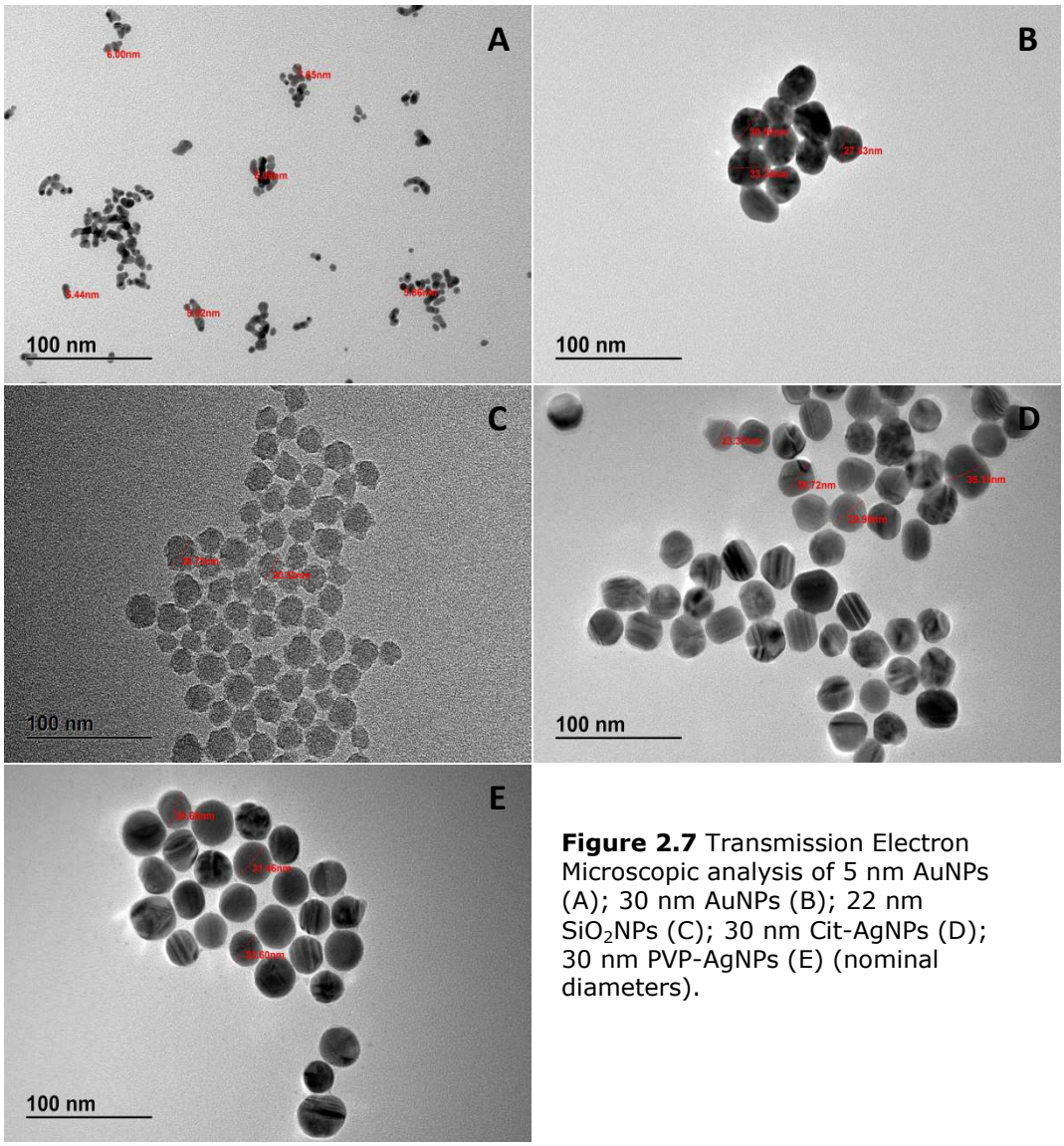

Figure 2.7 Transmission Electron Microscopic analysis of 5 nm AuNPs (A); 30 nm AuNPs (B); 22 nm SiO_2NPs (C); 30 nm Cit-AgNPs (D); 30 nm PVP-AgNPs (E) (nominal diameters).

3 Characterisation of nanoparticle stability in serum-containing cell culture media

In the previous sections the nanoparticle size distributions of the stock materials have been described as they are present in the simple dispersion or original synthesis media and without the presence of the proteins and salts which are vital components of the full cell culture media used in the validation test protocol. Under these conditions the particles are expected to be either fully dispersed (mainly single particles) as in the case of the selected materials or, in the case of suspensions derived from dried powders, to be a mixture of single particles and agglomerates/aggregates. The majority of particles in this study maintain their colloidal stability in their stock solution via electrostatic stabilisation which generally becomes less effective in the presence of dissolved ionic salts. At the salt concentration levels of cell culture media there is a high probability that a rapid and irreversible agglom of normally stable nanoparticles will occur. The presence of proteins may mitigate or exasperate the effect of salt depending on the nature of the particles and the proteins involved. Consequently, it is not generally possible to reliably predict how a certain type of particle will behave in any particular type of cell culture medium and thus it is generally advisable to determine this behaviour experimentally. In this study the colloidal stability of the test materials when exposed to different serum containing cell culture media has been qualitatively evaluated by using UV-Vis, DLS and CLS. A comparison was made between the samples immediately after dilution in water or serum-media mixture (time 0 hour) and after being held for 1, 4, 24 or 48 hours under standard cell culture conditions (5% CO_2, 95% humidity and 37°C). The composition of each complete culture media is described in Table 2 (Chapter 2.1). Results of the NPs physical-chemical characterisation in different complete culture media are reported specifically for each NP.

3.1 Description of characterisation methods

3.1.1 UV-Visible spectroscopy

UV-vis spectra were recorded with an EnSpire Multimode Plate Reader (Perkin Elmer) at 37 °C. The NPs were diluted in water or complete culture medium (without phenol red) at 37 °C at various final concentrations (5 nm AuNPs and 30 nm AuNPs : 300, 150, 75, 37.5 and 18.75 µM, 30 nm Cit-AgNPs and 30 nm PVP-AgNPs: 20, 10, 5, 2.5, 1.25 µg/mL). The suspensions were homogenized for 20 seconds using vortex and the absorption spectra of NPs was recorded immediately after dilution (0 hour) and after incubated for 1, 4, 24 or 48 hours under standard cell culture conditions (5% CO_2, 95% humidity and 37°C). The experiment was repeated twice in triplicates.

3.1.2 DLS measurements

Particle size distribution (PSD) of NPs was determined by DLS using a Zetasizer Nano-ZS instrument (Malvern Instruments Ltd, UK) with temperature control (25°C). The NPs were diluted in water or complete culture medium at 37 °C at various final concentrations (30 nm AuNPs: 300 µM, 22 nm SiO_2NPs: 1 and 0.1 mg/mL, 30 nm Cit-AgNPs and 30 nm PVP-AgNPs: 20 µg/mL). The suspensions were homogenized for 20 seconds using vortex and the particle size distribution of NPs was analyzed immediately after dilution (0 hour) and after incubation for 1, 4, 24 or 48 hours under standard cell culture conditions (5% CO_2, 95% humidity and 37°C). Each sample was recorded in quadruplicate after a temperature equilibration step of 120 sec. The instrument was set to automatic acquisition mode. Hydrodynamic diameters were calculated from the DLS intensity-weighted particle size distributions derived from NNLS fitting of the measured correlograms.

3.1.3 CLS measurements

Particle size distributions of NPs were determined by CLS using a CPS instrument (model DC24000UHR, CPS Instruments). The NPs were diluted in water or complete culture medium at 37 °C at various final concentrations (5 nm AuNPs and 30 nm AuNPs: 300, 100, 75 µM; 22 nm SiO2NPs: 1, 0.5 and 0.1 mg/mL; 30 nm Cit-AgNPs and 30 nm PVP-AgNPs: 20 and 10 µg/mL). The suspensions were homogenized for 20 seconds using vortex and the particle size distribution of NPs was analysed immediately after dilution (0 hour) and after incubation for 1, 4, 24 or 48 hours under standard cell culture conditions (5% CO2, 95% humidity and 37°C). Measurements were performed in an 8 wt% - 24 wt% sucrose density gradient at a disc speed of 22000 rpm. Each sample injection of 100 µL was preceded by a calibration step performed using certified poly(vinyl chloride) (PVC) particle size standard with a diameter of 239 nm (source?).

3.2 Results

3.2.1 Gold nanoparticles with diameter of 5 nm

The position of the absorption band maximum measured by UV–vis spectrometry (513 nm) was in agreement with the value expected for 5 nm diameter AuNPs diluted in water. This value was constant after 48 hours of incubation at 37 °C in water. The 5 nm AuNPs incubated in various complete culture media had a shift in the absorption band maximum to higher wavelengths and these values showed an increase during 48 hours. These results are reported as absorption spectra and peak shifts in time in Figure 3.1.and numerically as positions of the maxima of the plasmon resonance peaks in Table 3.1 for the highest tested particle concentration.

Table 3.1 Plasmon resonance peak position (nm) of 5 nm AuNPs in water and various culture media at 0, 1, 4, 24, 48 h time points after incubation at 300 µM concentration, at 37 °C.

Time	Water	F12+ 10%CS	DMEM+ 10%FBS	MEM+ 20%FBS	RPMI+ 10%HS
0 h	513	516	522	516	513
1 h	513	516	522	519	513
4 h	513	516	522	522	513
24h	513	522	534	522	534
48h	513	522	534	534	534

In case of such small NPs, the surface plasmon resonance (SPR) peak shifts of up to 21 nm were unlikely to be attributable the protein corona formation only. Indeed according to Mie theory, the decay length of the plasmon peak shift is very short for small particles (around 1-2 nm) resulting in a very low sensitivity to the protein thickness increases beyond this value. Even if a clear peak widening is observed, the measured SPR peak shift may be due to some possible NP agglomeration (formation of dimers) in particular for DMEM and RPMI.

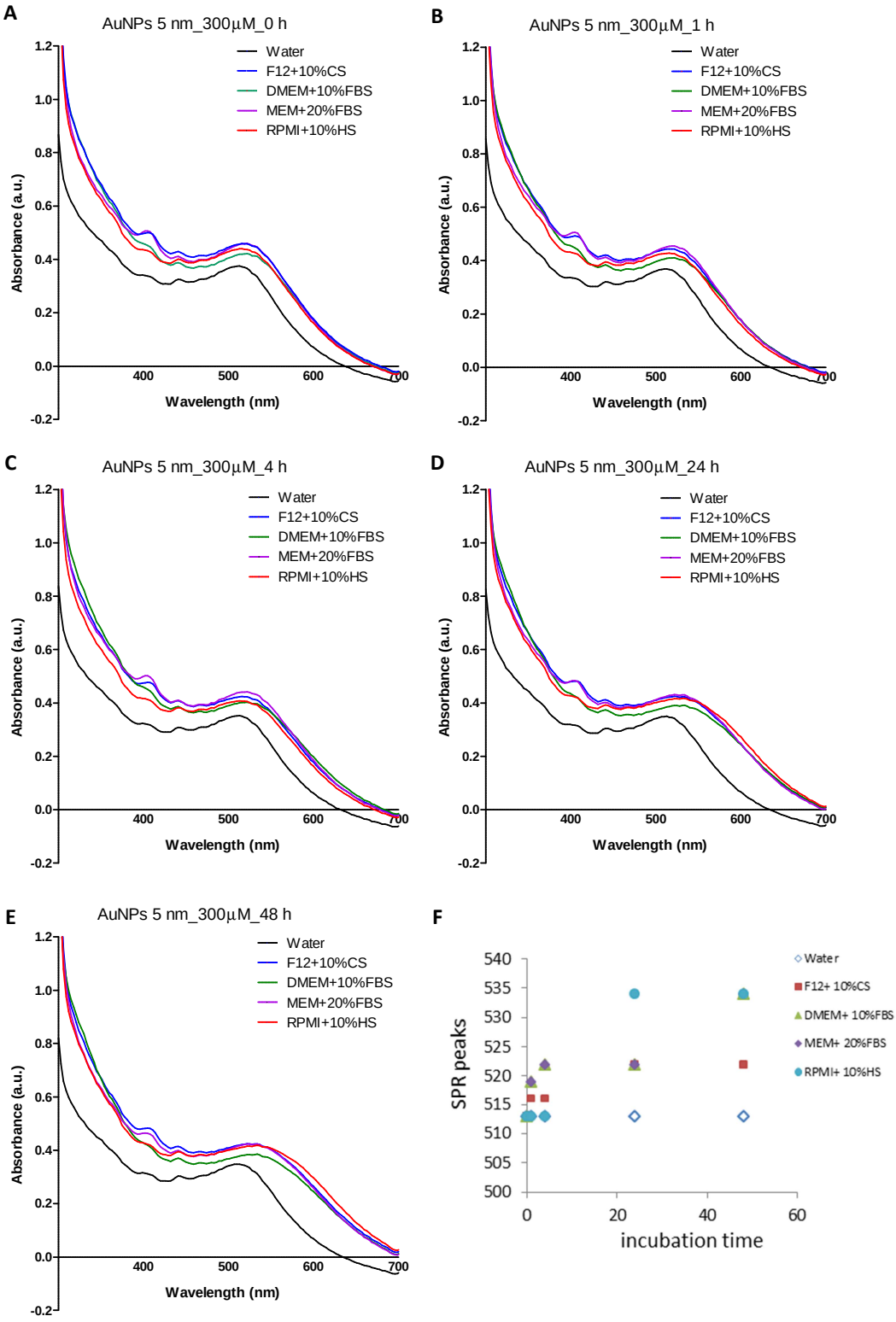

Figure 3.1 Absorption spectra of 5 nm AuNPs incubated in water or in various complete culture media at 300 µM concentration, at 37 °C for 0 (A), 1 (B), 4 (C), 24 (D) or 48 (E) hours; F) SPR peak position at various time points in the different culture media.

The moderate agglomeration of 5 nm AuNPs is confirmed by CLS showing somewhat widened mass based particle size distributions, with a tail at larger particle diameters compared to the particle size distribution in water. CLS results - at first sight - suggest a shift of particle size distribution modes to lower diameter values in serum containing culture media compared to water (Figure 3.2 A). This apparent decrease in the particle size can be explained by protein adsorption on the particles, which leads to decreased density and - as a consequence – longer sedimentation times. In standard computations using bulk gold densities, the longer sedimentation times will (incorrectly) result in lower calculated particle diameters. Considering also that the size of serum proteins is in a similar range as the size of these NPs (with diameter of the hydrated bovine serum albumin of about 6 nm) the change in particle size distributions and the shift of the mass based size distribution modes (Table 3.2.) in various culture media suggest the formation of only small agglomerates up to 24 hours at all tested particle concentrations.

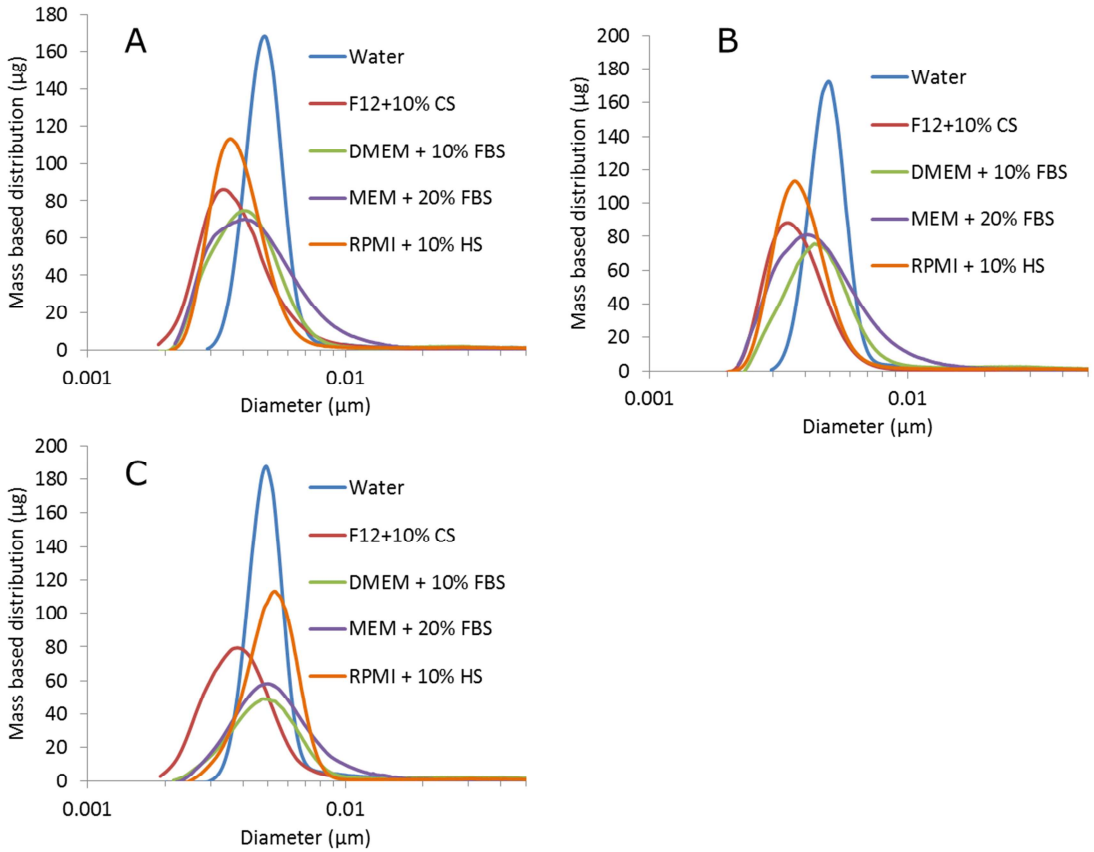

Figure 3.2 Mass based size distributions by CLS of 5 nm AuNPs incubated in water or in various culture media at 300 µM concentration, at 37 °C for 0 (A), 1 (B), or 24 (C) hours.

Table 3.2 Size distribution results by CLS for 5 nm AuNPs incubated in water or in various culture media at 37 °C for 0, 1 or 24 hours.

Size distribution by CLS (nm/HHW[1]/PdI[2])						
Au concentration (µM)	**Time (h)**	**Water**	**F12+ 10%CS**	**DMEM+ 10%FBS**	**MEM+ 20%FBS**	**RPMI+ 10%HS**
75	0	5/2/2.72	5/5/7.62	5/6/4.05	4/nd/7.34	5/6/3.83
	1	5/2/1.88	4/4/4.43	6/6/5.40	4/3/5.26	5/3/3.67
	24	6/3/3.05	4/4/3.98	6/5/5.34	4/2/5.33	8/5/3.27
100	0	5/2/2.34	4/nd/5.96	5/nd/3.76	6/8/4.61	4/5/2.41
	1	5/2/1.89	6/6/3.15	5/5/4.96	6/8/3.50	4/4/3.96
	24	5/2/2.40	5/7/3.39	5/5/4.69	6/7/3.47	5/4/3.98
300	0	5/2/1.38	3/3/2.20	4/3/2.23	5/4/2.13	4/2/1.96
	1	5/2/1.51	3/2/2.12	4/3/2.32	4/4/2.37	4/2/2.07
	24	5/2/1.51	4/3/2.66	5/4/2.43	4/4/1.77	5/3/2.00

[1]Half Height Width (HHW), [2]CLS Polydispersity Index (Dw/Dn) defined as the mean of mass based size distribution divided by the mean of number based size distribution; nd: not determined.

Particles with such small dimensions (<10 nm) cannot be properly characterised by DLS, because of the limitations of the method. The presence of serum proteins of similar size range in CCM further complicates the interpretation of DLS data. Therefore DLS results are not shown for 5 nm gold NPs in culture media.

3.2.2 Gold nanoparticles with diameter of 30 nm

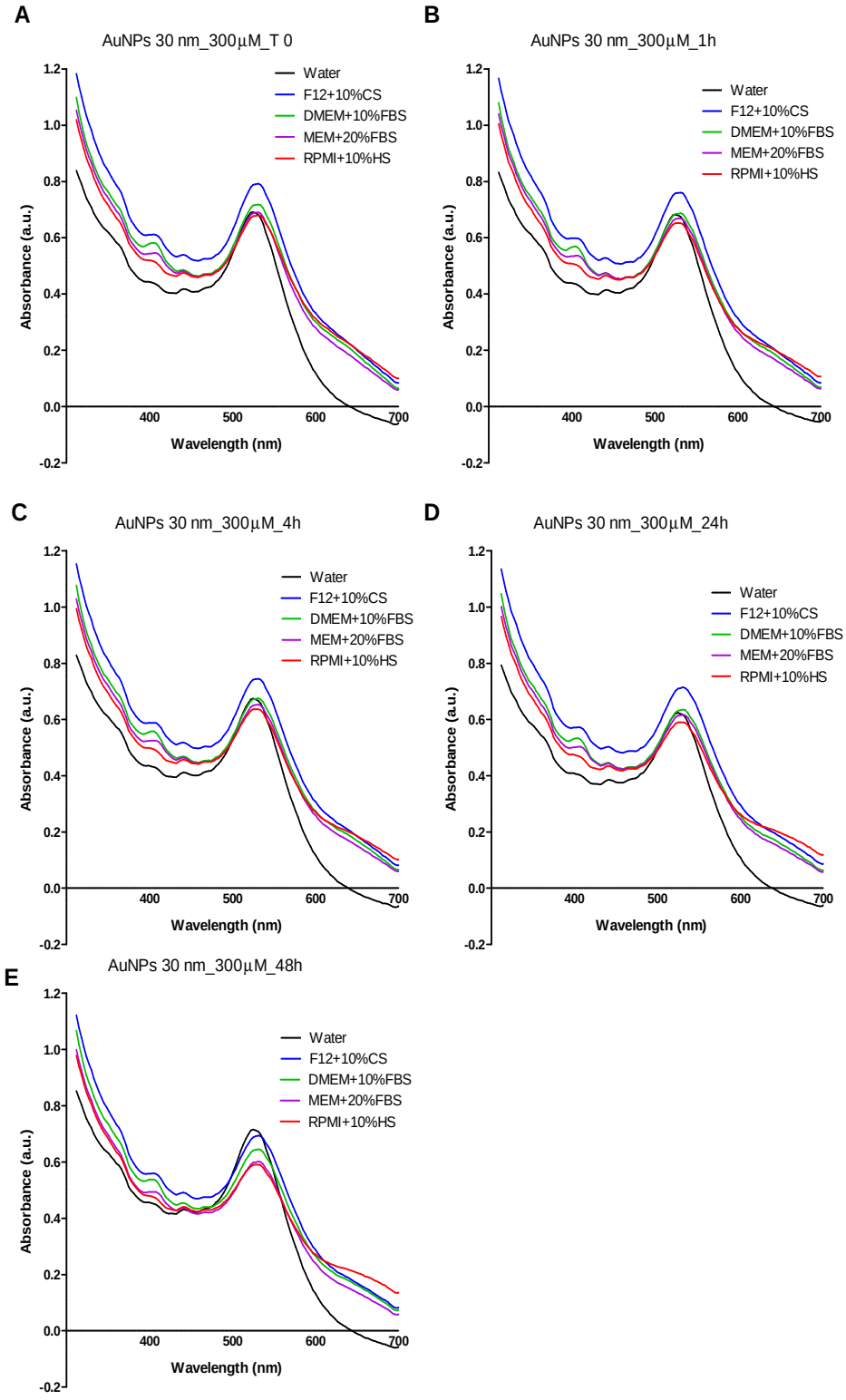

Figure 3.3 Absorption spectra of 30 nm AuNPs incubated in water or in various complete culture media at 300 µM concentration, at 37 °C for 0 (A), 1 (B), 4 (C), 24 (D) or 48 (E) hours.

Position of the absorption band maximum measured by UV–vis spectrometry (525 nm) was in agreement with the value expected for 30 nm diameter AuNPs diluted in water. This value was constant for 48 hours of incubation at 37 °C in water.

Table 3.3 Plasmon resonance peak position (nm) of 30 nm AuNPs in water and various culture media at 0, 1, 4, 24, 48 h time points after incubation at 300 μM concentration, at 37 °C.

Time	Water	F12+ 10%CS	DMEM+ 10%FBS	MEM+ 20%FBS	RPMI+ 10%HS
0 h	525	531	531	531	531
1 h	525	531	531	531	531
4 h	525	531	531	531	525
24h	525	531	531	531	531
48h	525	531	531	531	531

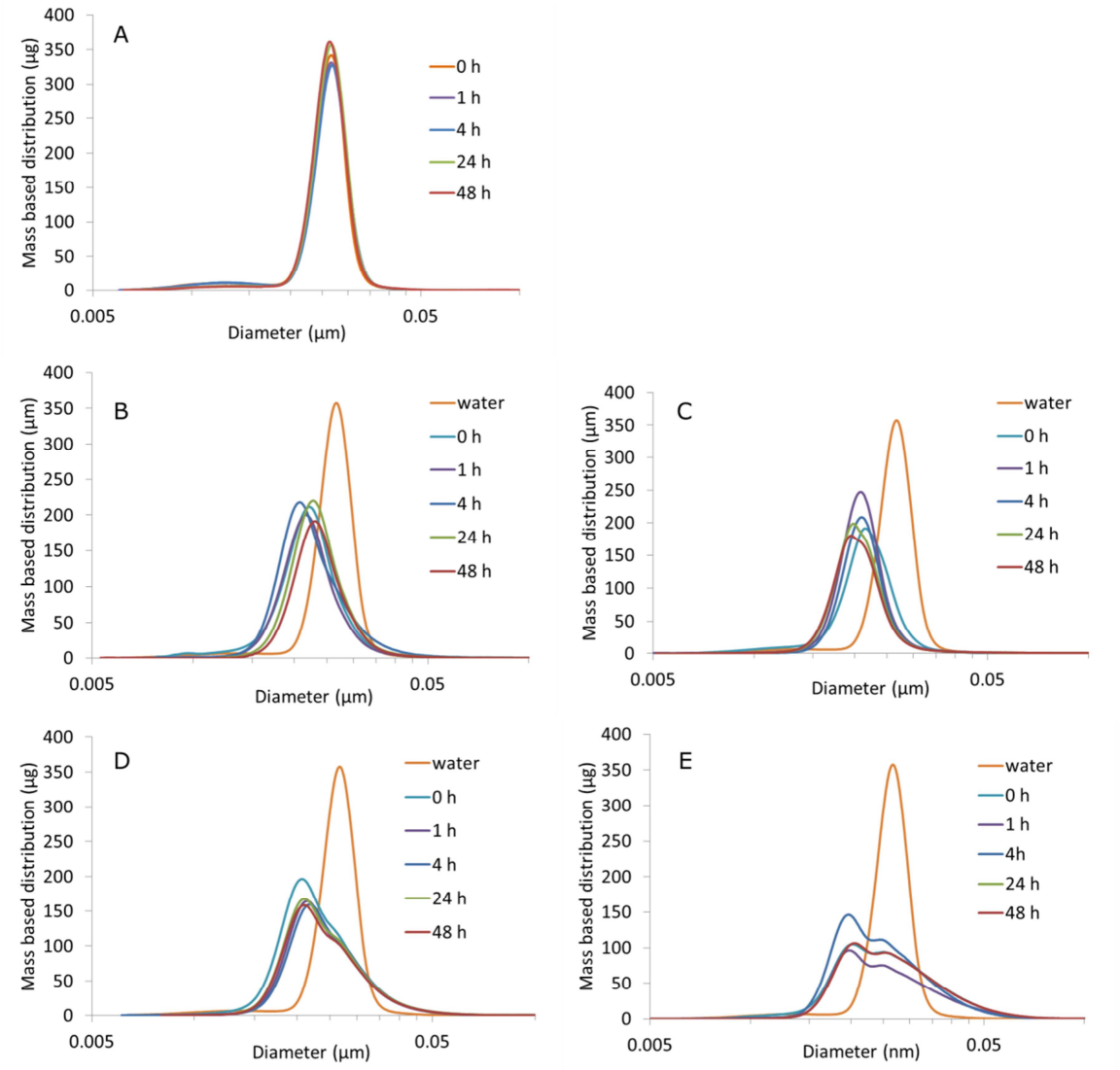

Figure 3.4 Mass based size distributions by CLS of 30 nm AuNPs incubated at 300 μM in (A) water, (B) F12+10%CS, (C) DMEM+10%FBS, (D) MEM+20%FBS or (E) RPMI+10%HS at 37 °C for 0, 1, 4, 24, 48 hours.

Incubation in various complete culture media resulted in a slight, immediate shift of the absorption band maximum to higher wavelengths (531 nm) with no further change up to 48 hours. These results are reported as absorption spectra in Figure 3.3 and numerically as positions of the maxima of the plasmon resonance peaks in Table 3.3 for the highest tested particle concentration.

The slight shift in the UV-Vis spectrum is most probably due to a moderate agglomeration of the particles in CCM. CLS measurements also confirm the formation of small agglomerates. As it is illustrated for the highest tested concentration in Figure 3.4, the particle size distribution of 30 nm Au NPS does not change in water for 48 hours. In serum containing media, the apparent particle diameter is decreased because of protein adsorption and corresponding density decrease. In parallel with this, size distributions are widened, and in case of MEM + 20% FBS and RPMI + 10% HS the size distribution becomes clearly multimodal, indicating the presence of dimers and small multimers. However, after the reaction with CCM components, size distributions do not change significantly with time up to 48 hours and do not depend on particle concentration in the investigated range (Table 3.4).

Table 3.4 Size distribution by CLS of AuNPs 30 nm incubated in water or in various culture media for 0, 1, 4, 24 or 48 hours.

Size distribution by CLS (nm/HHW[1]/PdI[2])						
Au concentration (μM)	Time (h)	Water	F12+ 10%CS	DMEM+ 10%FBS	MEM+ 20%FBS	RPMI+ 10%HS
75	0	26/8/1.64	23/13/1.57	22/7/1.35	22/7/1.72	20/7/1.63
	1	27/7/1.48	23/13/1.57	21/6/1.31	21/7/1.41	20/6/1.08
	4	27/7/1.61	22/13/1.28	21/6/1.21	20/7/1.42	20/6/1.16
	24	27/6/1.21	22/13/1.48	20/6/1.19	22/7/1.39	20/7/1.11
	48	26/7/1.21	24/13/1.41	20/6/1.31	21/7/1.25	19/7/1.21
100	0	26/6/1.57	23/10/1.30	22/7/1.94	22/9/1.32	20/9/1.26
	1	26/6/1.39	23/11/1.47	21/6/1.25	21/8/1.17	20/8/1.27
	4	26/6/1.47	23/11/1.42	21/6/1.13	21/8/1.18	20/11/1.19
	24	26/6/1.52	23/11/1.42	19/6/1.33	21/8/1.25	20/11/1.28
	48	25/6/1.42	23/11/1.49	19/6/1.30	21/8/1.27	20/11/1.36
300	0	27/7/1.41	22/8/1.34	21/7/1.46	22/8/1.37	20/6/1.21
	1	27/7/1.45	22/8/1.18	21/7/1.25	20/7/1.88	19/6/1.17
	4	27/7/1.41	23/8/1.26	21/6/1.16	22/7/1.18	21/6/1.26
	24	27/7/1.30	23/8/1.19	20/7/1.33	21/7/1.27	20/6/1.27
	48	26/7/1.24	23/8/1.17	20/7/1.28	20/6/1.15	20/6/1.29

[1]Half Height Width (HHW). [2]CLS Polydispersivity Index (Dw/Dn) defined as size distribution of NPs' weight divided by size distribution of the NPs' number.

During the DLS measurement series, these particles were sedimenting with the incubation time indicated by the dropping count rates (the amount of scattered light detected) shown in Figure 3.5 for the highest particle concentration. As the NPs sediment, the concentration of particles in the path of the laser light decreases, resulting in decreased count rates after 4 hours.

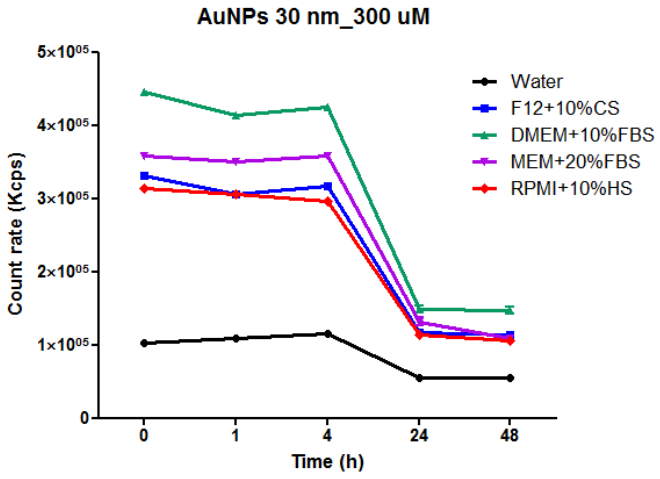

Figure 3.5 DLS count rates detected at various time points in the 300 μM suspension of 30 nm Au NPs in various culture media

Immediately after the reaction with serum proteins, the intensity based size distribution of the NPs was shifted to higher diameters as shown in Figure 3.6 at 0 h and 1 h. (Data were not collected for the same batch after longer times because of the drop in the detected count rate, i.e. particle sedimentation). In complete culture media a small peak appears at about 10 nm diameter – corresponding to the serum proteins present in the suspension. The mean hydrodynamic diameter of the particles (second, main peak in the figure) is shifted from 49 to about 80 nm accompanied by the widening of the peak - indicating protein adsorption and the formation of small agglomerates in CCM.

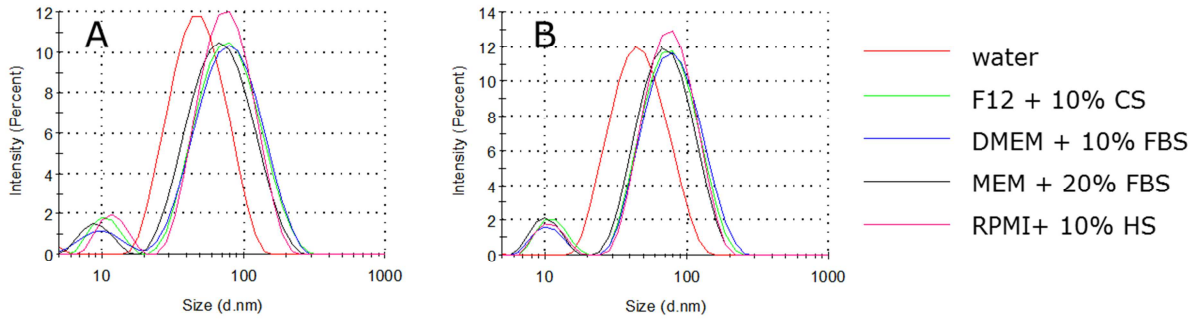

Figure 3.6 Intensity based size distributions (hydrodynamic diameter) of 30 nm Au NPs at (A) 0 h and (B) 1 h in water and in various culture media.

Recalculation of the CLS diameters considering the real density of particles originated from the core-shell structure of the protein coated, hydrated particles results in very similar 47 and 67-81 nm diameter values for the particles in water and in the various culture media, respectively.[2]

3.2.3 Silica nanoparticles with diameter of 22 nm

The density (~2.2 g/mL) of silica NPs synthesized by the method of Hartlen et al.[26] differs much less from the density of the hydrated protein corona than the density of bulk gold or silver. Consequently, the apparent shift of particle diameters to lower values described previously for 30 nm Au NPs is much less with silica and does not complicate data interpretation in CLS measurements. Silica NPs were stable in water for 48 hours at 37 °C (Figure 3.7 A). They reacted promptly with components of F12 +10%FCS and RPMI + 10%HS, showing fast agglomeration (widening of the size distribution curves) and a shift of the size modes to values above 100 nm (Figure 3.7 B,E; Table 3.5). The agglomeration of the silica NPs is slower, but still obvious in DMEM and MEM containing 10% FBS (Figure 3.7 C,D) suggesting that the serum component of the CCM plays a key role in the agglomeration process. As shown in Figure 3.8, neither serum free culture medium nor the 10% serum itself in water causes the size distribution shift.

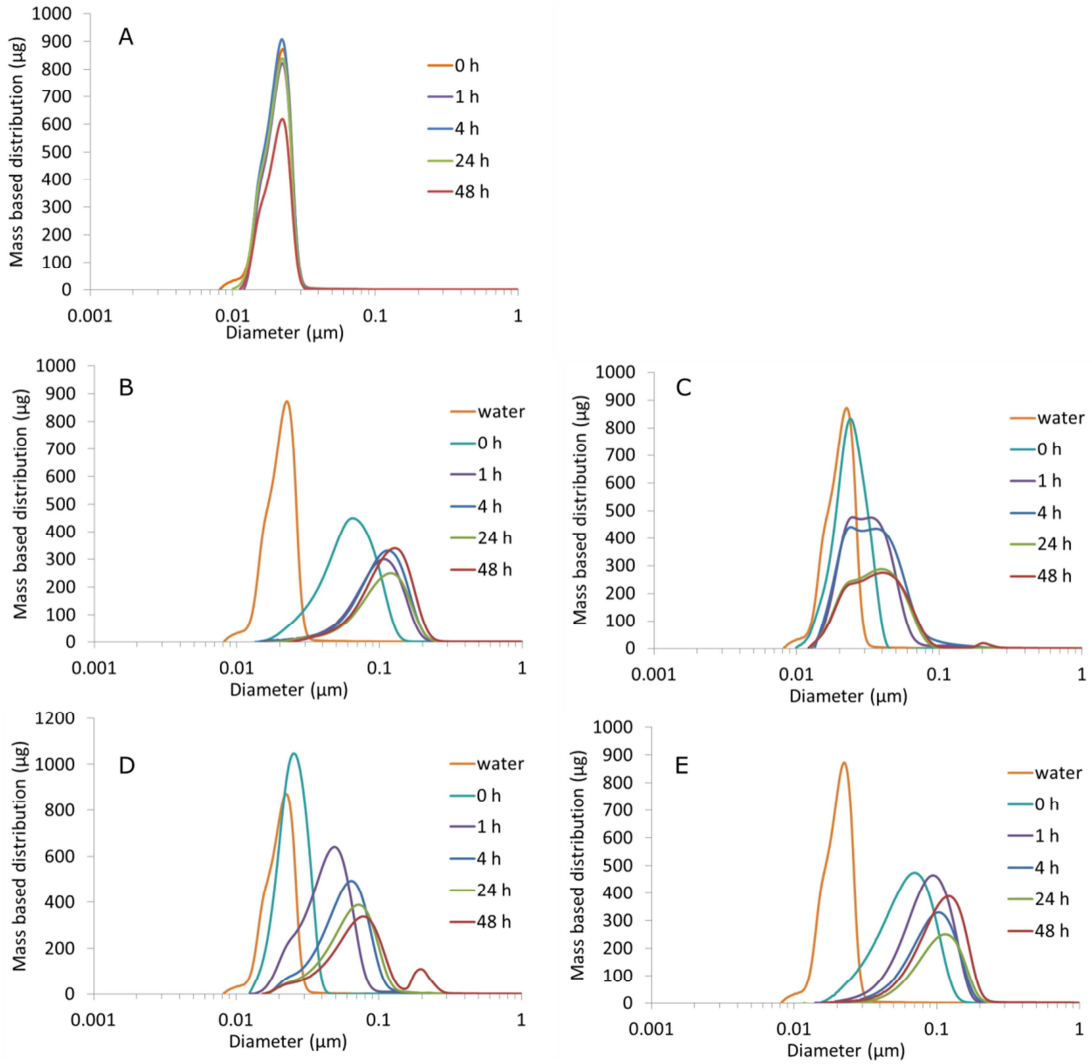

Figure 3.7 Size distribution by CLS of 22 nm SiO2 NPs incubated at 1 mg/mL concentration in (A) water, (B) F12+10%CS, (C) DMEM+10%FBS, (D) MEM+20%FBS or (E) RPMI+10%HS at 37 °C for 0, 1, 4, 24, 48 hours.

On the other hand, serum in culture media induces NP agglomeration depending on the composition (origin) of the serum. The process is also NP concentration dependent, with stronger agglomeration at higher particle concentrations (Table 3.5).

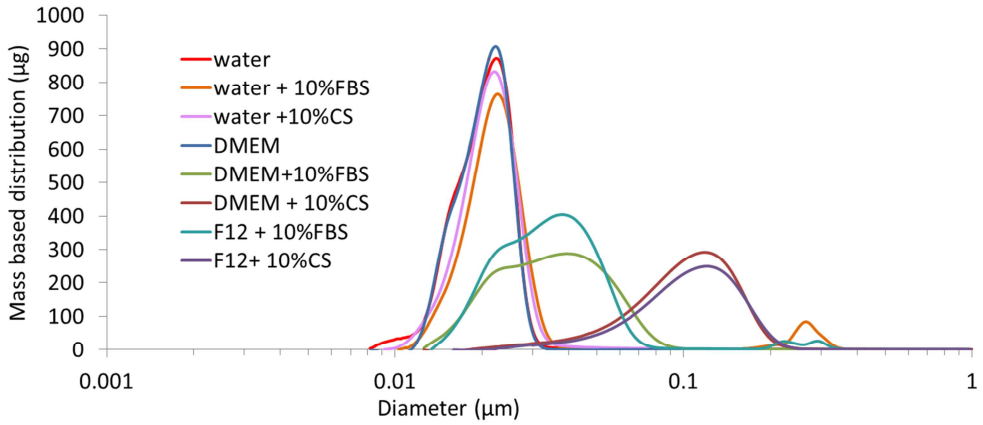

Figure 3.8 Size distribution by CLS of 22 nm SiO2 NPs incubated at 1 mg/mL concentration in water, water + 10% FBS, water + 10% CS, DMEM, DMEM+10%FBS, DMEM +10% CS, F12+ 10%FBS and F12+10%CS at 37 °C for 24 hours.

Table 3.5 Size distribution by CLS of 22 nm SiO_2NPs incubated in water or in different culture media (F12+10%CS, DMEM+10%FBS, MEM+20%FBS or RPMI+10%HS) at 0.1, 0.5 and 1 mg/mL concentration, at 37 °C for 0, 1, 4, 24 or 48 hours.

Size distribution by CLS (nm/HHW[1]/PdI[2])						
SiO_2 concentration (mg/mL)	Time (h)	Water	F12+ 10%CS	DMEM+ 10%FBS	MEM+ 20%FBS	RPMI+ 10%HS
0.1	0	23/9/1.21	37/44/2.16	27/28/1.30	22/15/1.20	22/10/1.14
	1	23/9/1.26	40/44/1.69	48/39/1.55	22/17/1.25	21/8/1.16
	4	23/10/1.32	40/40/1.59	61/51/1.64	23/16/1.26	21/6/1.45
	24	23/10/1.32	29/31/1.80	65/49/1.64	19/9/1.28	19/7/1.27
	48	22/11/1.37	26/18/2.59	39/36/1.68	16/7/1.52	16/4/3.61
0.5	0	22/11/1.16	40/33/1.48	26/16/1.30	26/16/1.64	40/37/1.49
	1	22/11/1.20	66/55/1.74	36/40/1.68	59/72/1.95	50/48/1.68
	4	22/10/1.51	73/61/1.73	40/41/1.75	64/nd/2.21	54/48/1.66
	24	22/11/1.18	94/83/1.71	45/40/2.03	64/84/2.24	90/72/1.62
	48	22/11/1.20	101/86/2.01	46/41/1.93	65/93/2.24	110/86/2.16
1	0	22/11/1.22	65/65/1.79	24/15/1.27	25/15/1.20	70/67/1.81
	1	22/11/1.14	108/81/2.03	33/30/1.46	49/38/1.56	93/82/1.78
	4	22/11/1.15	114/96/2.31	36/31/1.62	64/50/1.67	103/86/1.66
	24	22/11/1.16	120/100/1.99	39/45/1.64	73/58/1.82	115/94/1.54
	48	22/11/1.15	128/103/1.80	40/48/1.82	78/64/2.32	122/98/1.88

[1]Half Height Width (HHW). [2]CLS Polydispersity Index (Dw/Dn) defined as the mean of mass based size distribution divided by the mean of number based size distribution

The CLS based results are also confirmed by DLS. The more pronounced agglomeration at higher concentration (Figure 3.9 B) results in particle sedimentation leading to decreased detected count rates. Particle sedimentation in F12 + 10% CS and RPMI + 10%HS was visible to the naked eye.

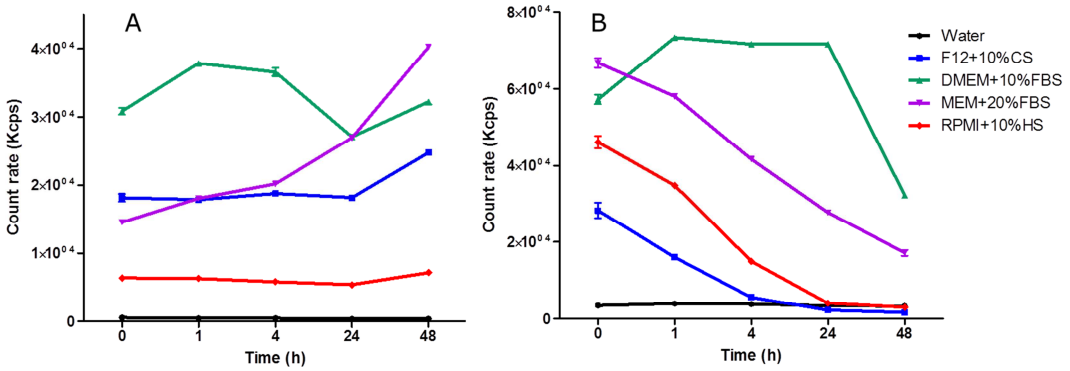

Figure 3.9 DLS count rates detected at various time points in the (A) 0.1 mg/mL and (B) 1 mg/mL suspension of 22 nm silica NPs in various culture media

The 22 nm SiO2NPs particles are stable in water for 48 h at 37°C at both investigated concentrations, and show prompt agglomeration in various serum containing culture media (Figure 3.10 A). The intensity based particle size distribution is shifted to higher diameters (MEM and DMEM in presence of FBS) or more peaks appear at higher sizes like in case of the RPMI + 10% HS and F12 +10%CS. At this point, most of the light arriving to the detector is scattered by the large agglomerates, therefore the calculated size distribution is dominated by these large particles and the Z-average value clearly indicates their presence (Table 3.6). At later time points (Figure 3.10 B) with the sedimentation of big particle agglomerates the serum proteins still in solution become the main light scattering component. As a result, zeta average values might decrease again (as in case of F12 +10%CS and RPMI+10%HS), but the PdI still indicates the polydisperse nature of the suspension (Table 3.6, last row).

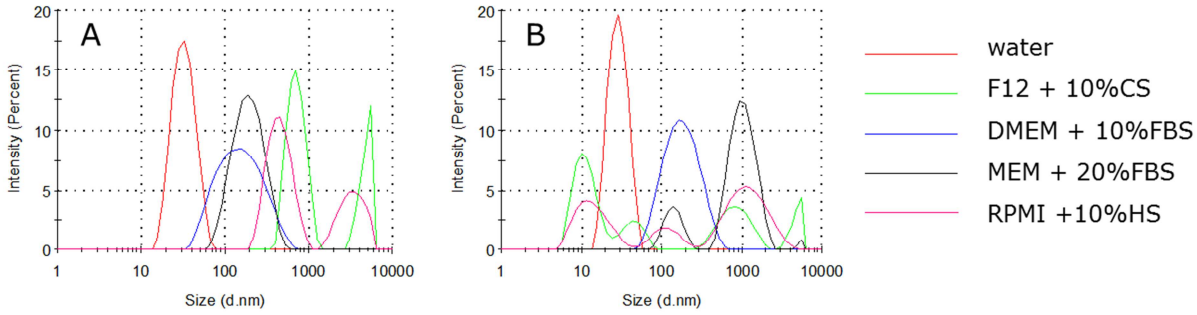

Figure 3.10 Intensity based size distributions (hydrodynamic diameter) of 22 nm silica NPs at 0 h (A) and 24 h (B) in water and in various culture media.

Table 3.6 Size distribution by DLS of 22 nm SiO_2NPs incubated in water or in different culture media at 0.1 and 1 mg/mL concentrations, at 37 °C for 0, 1, 4, 24 or 48 hours

Hydrodynamic diameter (Z-average in nm/PdI[1])						
SiO_2 concentration (mg/mL)	Time (h)	Water	F12+ 10%CS	DMEM+ 10%FBS	MEM+ 20%FBS	RPMI+ 10%HS
0.1	0	30.3/0.11	108.3/0.55	140.0/0.21	91.2/0.51	34.1/0.42
	1	28.7/0.09	101.0/0.52	157.4/0.19	99.1/0.41	32.1/0.43
	4	28.3/0.09	98.5/0.50	185.8/0.20	106.5/0.39	32.2/0.43
	24	27.8/0.09	102.7/0.48	244.4/0.41	160.0/0.25	34.0/0.42
	48	26.6/0.06	103.6/0.48	226.5/0.44	181.3/0.25	32.6/0.45
1	0	29.7/0.09	1295/0.38	128.3/0.23	175.5/0.25	697.9/0.54
	1	28.7/0.08	1237/0.82	146.5/0.22	284.2/0.34	1263/0.58
	4	27.7/0.07	584.2/0.79	154.8/0.24	316.7/0.38	790.4/0.90
	24	27.2/0.07	62.42/0.50	151.7/0.23	483.4/0.53	72.41/0.89
	48	27.0/0.06	18.3/0.47	149.1/0.22	289.0/0.62	33.8/0.68

[1]DLS Polydispersity Index

3.2.4 Citrate stabilised silver nanoparticles with diameter of 30 nm

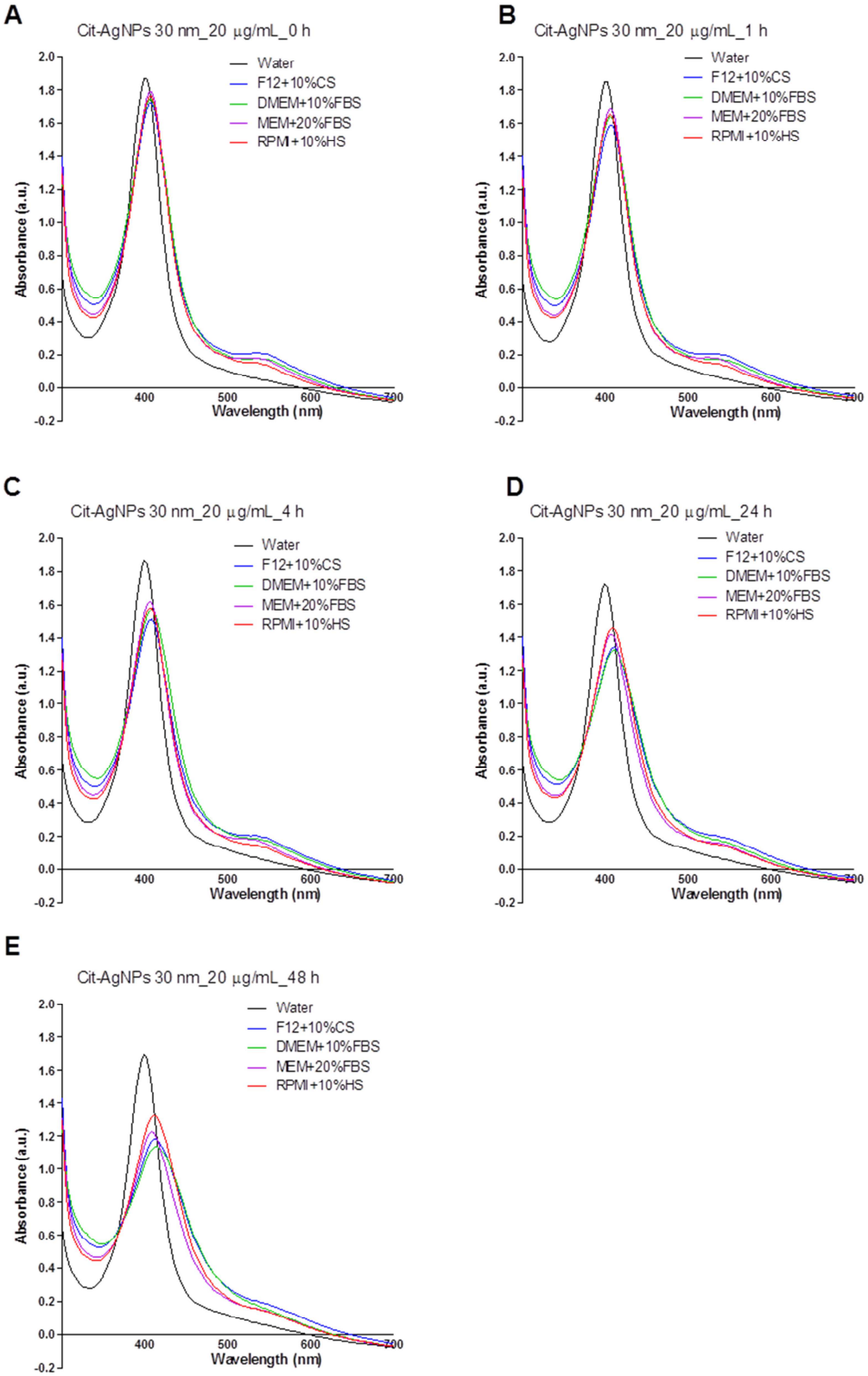

Figure 3.11 Absorption spectra of 30 nm Cit-AgNPs incubated in water or in different complete culture media at 37 °C for 0 (A), 1 (B), 4 (C), 24 (D) or 48 (E) hours.

Position of the absorption band maximum measured by UV–vis spectrometry (402 nm) was in agreement with the value expected for 30 nm diameter AgNPs diluted in water. This value was constant for 48 hours of incubation at 37 °C in water. Incubation in various complete culture media resulted in a slight, immediate shift of the absorption band maximum to higher wavelengths (to 405-408 nm) with further slow increase up to 48 hours. These results are reported as absorption spectra in Figure 3.11 and numerically as positions of the maxima of the plasmon resonance peaks in Table 3.7 for the higher tested (20 µg/mL) concentration.

UV-Vis results suggest the formation of small particle agglomerates in serum containing media.

Table 3.7. Maximum position of the plasmon resonance peak (nm) of 30 nm Cit-AgNPs in water and various culture media at 20 µg/mL concentration, 37 °C, after 0, 1, 4, 24, 48 h incubation times.

Time	Water	F12+ 10%CS	DMEM+ 10%FBS	MEM+ 20%FBS	RPMI+ 10%HS
0 h	402	408	408	408	405
1 h	402	408	405	405	405
4 h	399	408	408	405	405
24h	399	411	411	408	408
48h	399	411	414	408	411

CLS measurements support this finding, showing widening of the size distribution peaks (Figure 3.12), increase of the polydispersity index (Table 3.8) and – similarly to Au NPs – a shift of the first size distribution mode to lower values because of the density decrease due to protein corona formation. In case of DMEM+10%FBS, MEM+20%FBS and RPMI+10%HS the peaks belonging to dimers and small multimers can be also well observed as shoulders of the main peak at higher diameters (Figure 3.12 C,D,E).

Similarly to the 30 nm AuNPs, the citrate stabilised silver nanoparticles of similar size (and their small agglomerates) do not show sedimentation neither in water nor in complete CCM. DLS count rates remained stable (did not decrease) for 48 h as illustrated by Figure 3.13 for the higher tested concentration. A moderate increase of hydrodynamic diameter was detected by DLS even in water with time (Table 3.9) most probably indicating the formation of dimers. Intensity based size distribution means of the particles measured by DLS immediately increase in CCM from 39 nm to 85-170 nm depending on culture medium (Figure 3.14). Further strong agglomeration cannot be observed by DLS in any of the media at 20 µg/mL Cit-AgNP concentration.

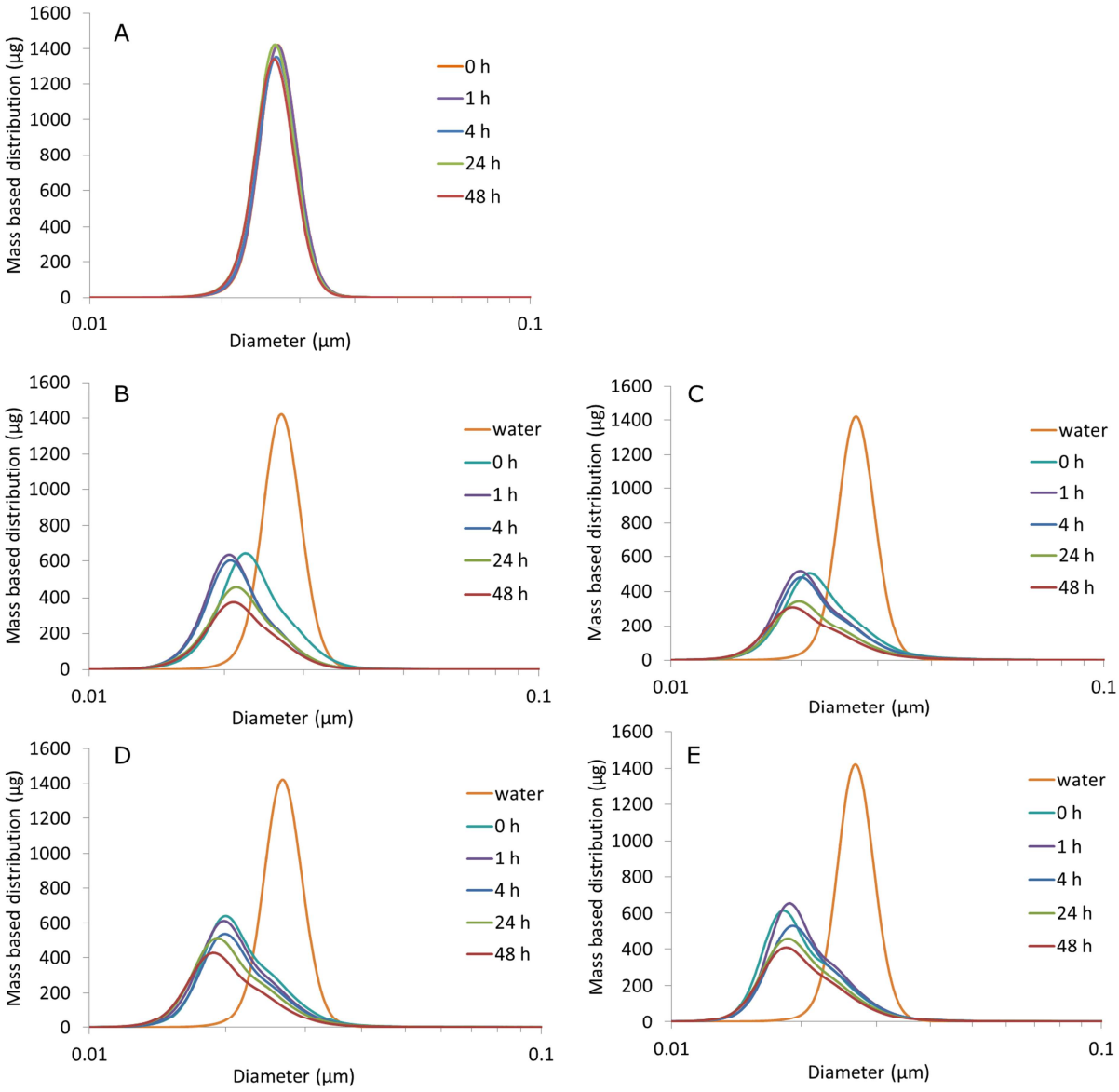

Figure 3.12 Size distribution by CLS of 30 nm Cit-AgNPs incubated at 20 µg/mL concentration in (A) water or in (B) F12+10%CS, (C) DMEM+10%FBS, (D) MEM+20%FBS and (E) RPMI+10%HS at 37 °C for 0, 1, 4, 24 and 48 hours.

The calculated size distributions (Figure 3.13) are multimodal, with a small peak appearing at about 10 nm due to the presence of serum proteins in the CCM. Thus, Z-average values reported in Table 3.9 have to be interpreted critically, as they reflect the average hydrodynamic diameter of a multimodal distribution. Nevertheless, the higher Z-averages together with the increased polydispersivity index values confirm the formation of small agglomerates detected by CLS measurements.

Table 3.8 Size distribution by CLS of Cit-AgNPs 30 nm incubated with water or with different culture media. Cit-AgNPs 30 nm (10 and 20 µg/mL) were incubated with water, F12+10%CS, DMEM+10%FBS, MEM+20%FBS or RPMI+10%HS at 37 °C for 0, 1, 4, 24 or 48 hours and after the size distribution was evaluated by CLS.

Size distribution by CLS (nm/HHW[1]/PdI[2])						
Ag concentration (µg/mL)	**Time (h)**	**Water**	**F12+10%CS**	**DMEM+ 10%FBS**	**MEM+ 20%FBS**	**RPMI+ 10%HS**
10	0	26/7/1.10	21/7/1.16	22/9/1.20	21/9/1.18	20/7/1.17
	1	26/7/1.09	21/7/1.15	20/9/1.18	20/8/1.15	20/7/1.15
	4	26/7/1.09	21/7/1.16	20/9/1.21	20/8/1.21	19/7/1.16
	24	26/6/1.08	20/8/1.17	20/10/1.23	19/8/1.18	18/8/1.21
	48	26/7/1.08	21/8/1.18	19/9/1.30	18/9/1.31	18/8/1.28
20	0	27/6/1.06	22/8/1.20	21/8/1.22	20/8/1.18	18/7/1.18
	1	27/6/1.06	21/7/1.14	20/8/1.17	20/7/1.15	19/7/1.15
	4	27/6/1.06	21/7/1.15	20/8/1.17	20/7/1.16	19/8/1.18
	24	27/6/1.09	21/8/1.19	20/8/1.23	19/8/1.20	19/8/1.20
	48	26/6/1.08	21/8/1.20	19/9/1.26	19/8/1.19	18/8/1.22

[1]Half Height Width (HHW).
[2]CLS Polydispersity Index (Dw/Dn) defined as the mean of mass based size distribution divided by the mean of number based size distribution

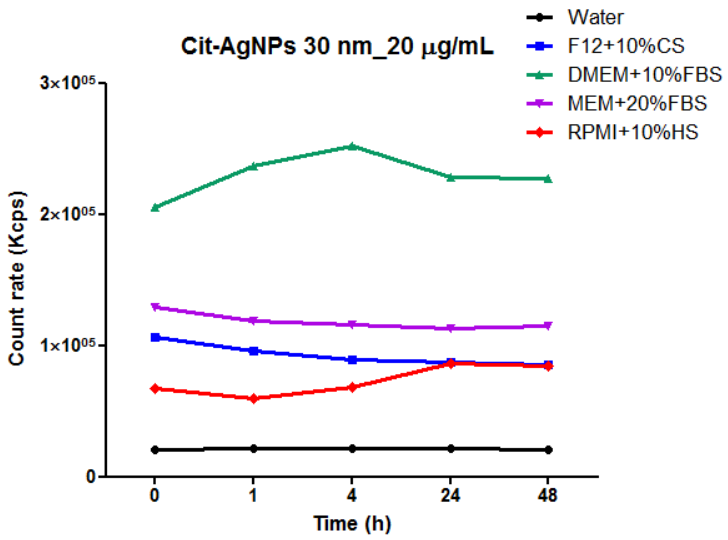

Figure 3.13 DLS count rates detected at various time points in the 20 µg/mL suspension of 30 nm Cit-AgNPs in various culture media

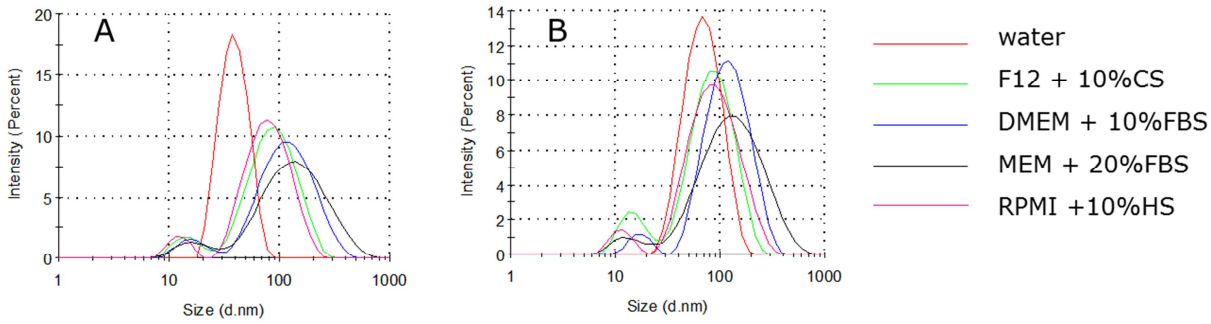

Figure 3.14 Intensity based size distributions (hydrodynamic diameter) of 30 nm Cit-AgNPs at (A) 0 h and (B) 48 h in water and in various culture media.

Table 3.9. Size distribution by DLS of Cit-AgNPs 30 nm incubated in water or in various culture media at 37 °C for 0, 1, 4, 24 or 48 hours.

		Hydrodynamic diameter (Intensity peak mean in nm/PdI[1])				
Ag concentration (µg/mL)	**Time (h)**	**Water**	**F12+ 10%CS**	**DMEM+ 10%FBS**	**MEM+ 20%FBS**	**RPMI+ 10%HS**
20	0	40.2/0.11	94.6/0.28	132.4/0.35	169.4/0.49	84.1/0.28
	1	40.1/0.09	87.7/0.30	127.0/0.29	180.9/0.46	82.1/0.29
	4	40.0/0.10	87.3/0.30	124.4/0.28	170.8/0.45	88.1/0.29
	24	68.7/0.23	84.6/0.35	126.8/0.27	156.9/0.46	93.1/0.29
	48	73.2/0.23	88.5/0.33	128.6/0.26	160.0/0.45	96.3/0.29

[1]DLS Polydispersity Index

3.2.5 PVP coated silver nanoparticles with diameter of 30 nm

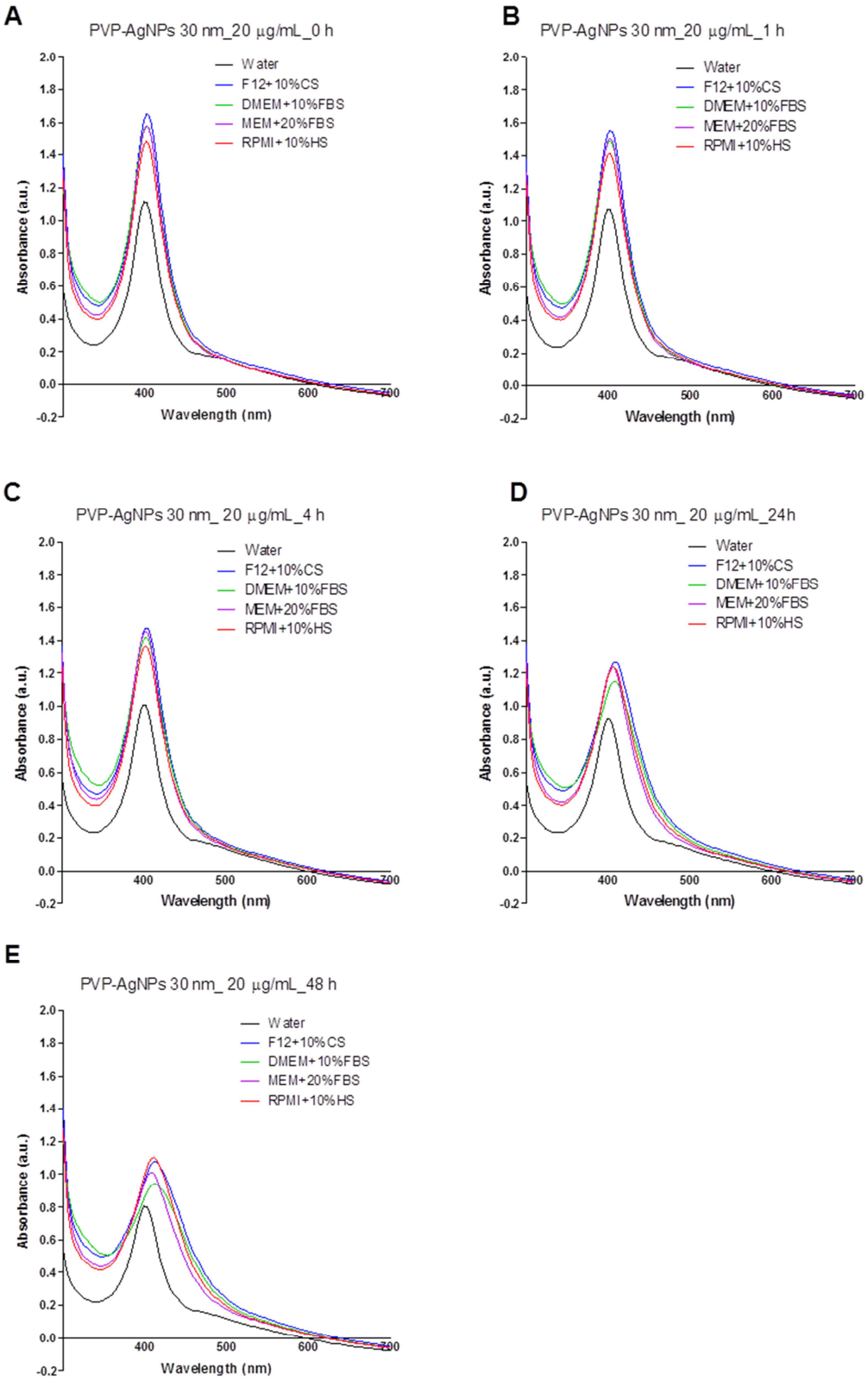

Figure 3.15 Absorption spectra of 30 nm PVP-AgNPs incubated in water or in different complete culture media at 37 °C for 0 (A), 1 (B), 4 (C), 24 (D) or 48 (E) hours.

UV-Vis absorption profile of the 30 nm PVP-AgNPs in water was found to be very similar to the Cit-AgNPs, having an absorption maximum at the expected wavelength. According to the plasmonic peak position (Figure 3.15. and Table 3.7.) they are stable in all tested CCM up to 24 h and show a slight shift of the peak position after 24 hours.

Table 3.7. Maximum position of the plasmon resonance peak (nm) of 30 nm PVP-AgNPs in water and various culture media at 20 µg/mL concentration, 37 °C, after 0, 1, 4, 24, 48 h incubation times.

Time	Water	F12+ 10%CS	DMEM+ 10%FBS	MEM+ 20%FBS	RPMI+ 10%HS
0 h					
1 h	399	402	402	402	402
4 h	399	402	402	402	402
24h	399	408	408	405	408
48h	399	411	411	408	411

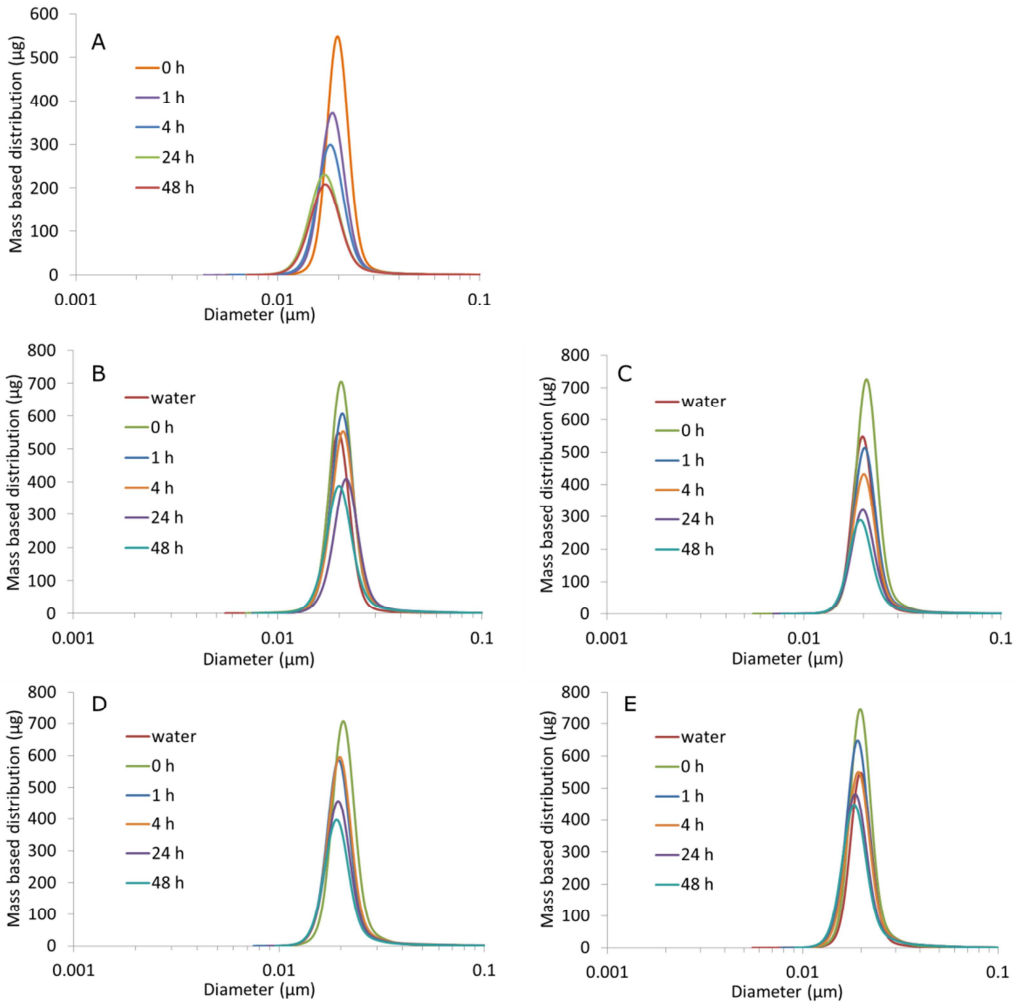

Figure 3.16 Size distribution by CLS of 30 nm PVP-AgNPs incubated at 20 µg/mL concentration in (A) water or in (B) F12+10%CS, (C) DMEM+10%FBS, (D) MEM+20%FBS and (E) RPMI+10%HS at 37 °C for 0, 1, 4, 24 and 48 hours.

PVP-AgNPs appear to be smaller than expected in CLS measurements (Figure 3.16 and Table 3.8) at a diameter of about 20 nm. As TEM images and UV-Vis spectra both confirm the nominal diameter, this observation can be explained by the presence of the hydrated polymer coating that can remarkably decrease the total density of the 30 nm silver particles. The Stokes diameter measured by CLS seems to be further decreasing with time in water (Figure 3.16 A) what can be most probably also attributed to the changes (swelling) of the PVP coating. The 30 nm PVP-AgNPs do not show notable agglomeration in any of the complete CCM, the detected diameter, peak with and polydispersity values remained stable for 48 hours in all tested media (Table 3.8).

Table 3.8 Size distribution by CLS of PVP-AgNPs 30 nm incubated in water or in various culture media at 37 °C for 0, 1, 4, 24 or 48 hours.

Size distribution by CLS (nm/HHW[1]/PdI[2])						
Ag concentration (µg/mL)	**Time (h)**	**Water**	**F12+10%CS**	**DMEM+ 10%FBS**	**MEM+ 20%FBS**	**RPMI+ 10%HS**
10	0	19/6/1.15	20/6/1.21	20/6/1.19	20/6/1.18	20/6/1.16
	1	19/6/1.16	21/6/1.17	20/6/1.24	20/6/1.18	20/8/1.20
	4	20/6/1.16	21/7/1.22	20/6/1.28	19/6/1.19	20/7/1.19
	24	19/6/1.16	20/7/1.20	19/6/1.32	18/6/1.28	18/8/1.37
	48	19/6/1.14	19/7/1.23	18.6/1.42	18/6/1.27	18/8/1.27
20	0	20/6/1.12	20/6/1.19	21/6/1.16	21/6/1.14	20/6/1.14
	1	19/6/1.14	21/6/1.15	20/6/1.18	19/6/1.18	19/6/1.14
	4	18/6/1.18	21/6/1.17	20/6/1.19	20/6/1.18	19/6/1.15
	24	17/7/1.31	22/7/1.22	20/6/1.23	19/6/1.17	19/6/1.17
	48	17/7/1.26	20/7/1.21	19/6/1.23	19/6/1.21	18/6/1.18

[1]Half Height Width (HHW).
[2]CLS Polydispersity Index (Dw/Dn) defined as the mean of mass based size distribution divided by the mean of number based size distribution

In accordance with the UV-Vis and CLS data, DLS measurements indicate that the 30 nm PVP-AgNPs are stable in culture media. No drop of the count rates was observed in any of the CCM for 48 hours. Hydrodynamic diameter (intensity based mean of the strongest peak) of the particles in water was about 80 nm and remained stable during the experiment. The quite high polydispersity index and a small peak appearing at about 10 nm might be explained by the release of free PVP from the particles. The possible PVP release emphasizes the importance of testing also the effect of solvents and stabilisers in the next *in vitro* test development phase of the project.

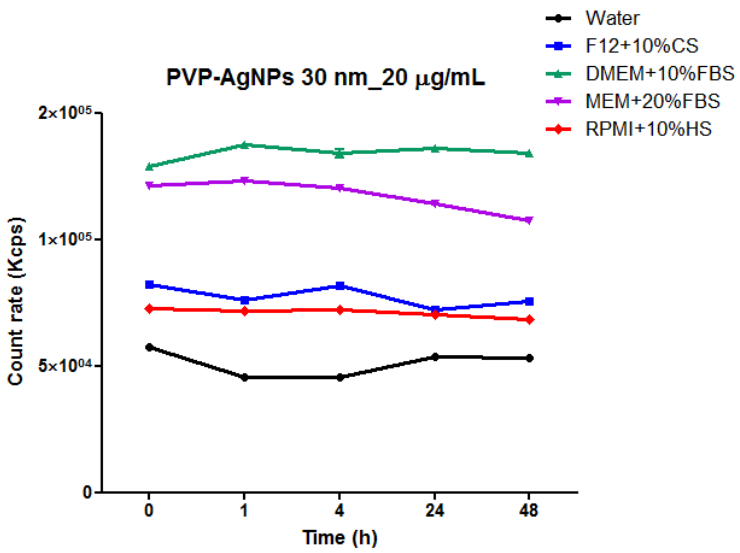

Figure 3.17 DLS count rates detected at various time points in the 20 µg/mL suspension of 30 nm PVP-AgNPs in various culture media

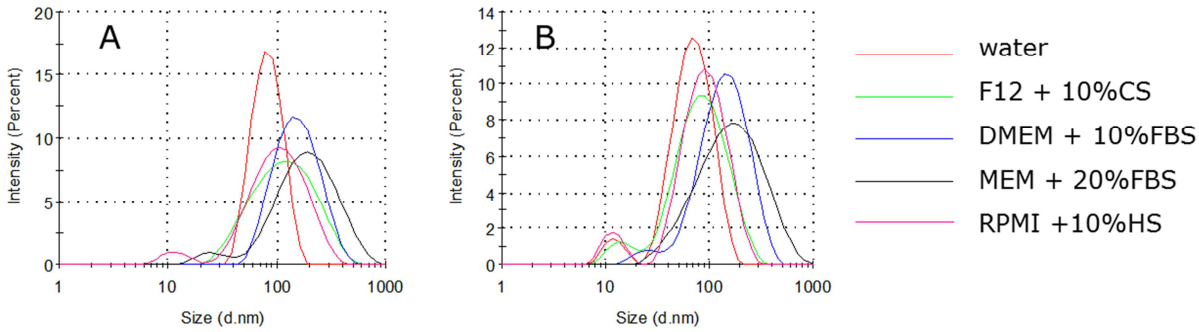

Figure 3.18 Intensity based size distributions (hydrodynamic diameter) of 30 nm PVP-AgNPs at (A) 0 h and (B) 48 h in water and in various culture media.

In complete culture media also serum proteins contribute to the polydispersity of the samples. Therefore intensity based means of the main peaks (Figure 3.18) better represent the hydrodynamic diameter of these NPs than Z-average values (Table 3.9). In CCM the diameter of the particles immediately increases from 80 nm to 110-210 nm depending on the medium. The largest change can be observed for MEM and DMEM containing 20% and 10% FBS, respectively (Figure 3.18). After the initial interaction with the medium (absorption of serum proteins), particle diameters did not show notable size change during the experiment. The 30 nm PVP-AgNPs are stable in CCM also according to the DLS measurements.

Table 3.9 Size distribution by DLS of 30 nm PVP-AgNPs incubated in water or in different culture media at 20 µg/mL concentration, at 37 °C for 0, 1, 4, 24 or 48 hours.

		Hydrodynamic diameter (Intensity peak mean in nm/PdI[1])				
Ag concentration (µg/mL)	**Time (h)**	**Water**	**F12+10%CS**	**DMEM+ 10%FBS**	**MEM+ 20%FBS**	**RPMI+ 10%HS**
20	0	84.3/0.20	127.0/0.40	160.0/0.25	212.9/0.41	113.3/0.40
	1	80.2/0.18	98.8/0.42	152.4/0.26	205.6/0.40	97.6/0.40
	4	81.3/0.24	105.6/0.42	155.7/0.27	208.6/0.35	101.2/0.40
	24	80.0/0.33	96.3/0.41	153.2/0.25	198.9/0.36	105.4/0.40
	48	74.3/0.36	96.3/0.41	154.2/0.26	194.8/0.41	104.2/0.41

[1]DLS Polydispersity Index

4 Conclusions

Physico-chemical characterisation of the synthesised and commercially sourced nanomaterials samples confirmed that the prepared stock suspensions contained equiaxial, mostly nearly-spherical nanoparticles with dimensions very close to the nominal particle size and with good monomodal size distribution. Experiments on the stock suspensions demonstrated that none of the single characterisation techniques is able to provide complete information on the samples. Therefore, several techniques were applied to observe the behaviour of the selected representative nanoparticles in complete CCM.

Most of the tested samples exhibited some kind of agglomeration in serum containing CCM – dependent also on the composition of the medium and the origin of serum. Only the PVP functionalised AgNP sample showed the type of size distribution change in culture media that could be attributed solely to protein adsorption without notable agglomeration. SiO_2 NPs were proven to be the most sensitive to interaction with serum containing CCM. The time and concentration dependent agglomeration of these particles was confirmed by both CLS and DLS measurements and in some cases the sedimentation of the large agglomerates generated was visible to the naked eye. In the case of 5 nm AuNPs, 30 nm AuNPs and 30 nm Cit-AgNPs the mild agglomeration led to the formation of dimers and small multimers and sedimentation of the 30 nm AuNPs was also observed. Table 4.1 summarises the information collected by the different methods about the behaviour of the samples (at the highest tested concentration) and the conclusions based on the comparative analysis of the data.

Table 4.1 Observations collected about the behaviour of the tested nanoparticles in serum containing complete cell culture media

Sample	**Methods**			**Conclusion**
	UV-Vis	CLS	DLS	
5 nm AuNPs	small agglomerates	small agglomerates	N.A.	mild agglomeration in CCM
30 nm AuNPs	small agglomerates	small agglomerates	prompt interaction with CCM sedimentation after 4 h	interaction with all tested CCM, mild agglomeration and particle sedimentation
22 nm SiO_2NPs	N.A.	agglomeration affected mainly by serum component	large agglomerates sedimentation	fast agglomeration and sedimentation depending also on CCM composition
30 nm Cit-AgNPs	small agglomerates	small agglomerates	small agglomerates no sedimentation	mild agglomeration generating small stable agglomerates
30 nm PVP-AgNPs	stable	stable	size shift depending on CCM composition	stable in all CCM for 48 h, possible PVP release

5 References

1. B. Halamoda-Kenzaoui, M. Ceridono, P. Colpo, A. Valsesia, P. Urbán, I. Ojea-Jiménez, S. Gioria, D. Gilliland, F. Rossi and A. Kinsner-Ovaskainen, *PLoS ONE,* 2015, 10, e0141593.

2. G. Rischitor, M. Parracino, R. La Spina, P. Urbán, I. Ojea-Jiménez, E. Bellido, A. Valsesia, S. Gioria, R. Capomaccio, A. Kinsner-Ovaskainen, D. Gilliland, F. Rossi and P. Colpo, *Particle and Fibre Toxicology*, 2016, 13, 47.

3. *European Commission, Journal*, 2011/696/EU.

4. R. Coradeghini, S. Gioria, C. P. Garcia, P. Nativo, F. Franchini, D. Gilliland, J. Ponti and F. Rossi, *Toxicol Lett*, 2013, 217, 205-216.

5. I. De Angelis, F. Barone, A. Zijno, L. Bizzarri, M. T. Russo, R. Pozzi, F. Franchini, G. Giudetti, C. Uboldi, J. Ponti, F. Rossi and B. De Berardis, *Nanotoxicology*, 2013, 7, 1361-1372.

6. I. Fenoglio, J. Ponti, E. Alloa, M. Ghiazza, I. Corazzari, R. Capomaccio, D. Rembges, S. Oliaro-Bosso and F. Rossi, *Nanoscale*, 2013, 5, 6567-6576.

7. K. Fujita, M. Fukuda, S. Endoh, H. Kato, J. Maru, A. Nakamura, K. Uchino, N. Shinohara, S. Obara, R. Nagano, M. Horie, S. Kinugasa, H. Hashimoto and A. Kishimoto, *Toxicol Mech Methods*, 2013, 23, 598-609.

8. A. Casey, E. Herzog, M. Davoren, F. M. Lyng, H. J. Byrne and G. Chambers, *Carbon*, 2007, 45, 1425-1432.

9. X. Han, R. Gelein, N. Corson, P. Wade-Mercer, J. Jiang, P. Biswas, J. N. Finkelstein, A. Elder and G. Oberdorster, *Toxicology*, 2011, 287, 99-104.

10. A. L. Holder, R. Goth-Goldstein, D. Lucas and C. P. Koshland, *Chem Res Toxicol*, 2012, 25, 1885-1892.

11. G. J. Oostingh, E. Casals, P. Italiani, R. Colognato, R. Stritzinger, J. Ponti, T. Pfaller, Y. Kohl, D. Ooms, F. Favilli, H. Leppens, D. Lucchesi, F. Rossi, I. Nelissen, H. Thielecke, V. F. Puntes, A. Duschl and D. Boraschi, *Part Fibre Toxicol*, 2011, 8, 8.

12. N. A. Monteiro-Riviere, A. O. Inman and L. W. Zhang, *Toxicol Appl Pharmacol*, 2009, 234, 222-235.

13. V. Stone, H. Johnston and R. P. Schins, *Crit Rev Toxicol*, 2009, 39, 613-626.

14. A. Kroll, M. H. Pillukat, D. Hahn and J. Schnekenburger, *Arch Toxicol*, 2012, 86, 1123-1136.

15. J. Ponti, R. Colognato, H. Rauscher, S. Gioria, F. Broggi, F. Franchini, C. Pascual, G. Giudetti and F. Rossi, *Toxicol Lett*, 2010, 197, 29-37.

16. *OECD, Preliminary Review of OECD Test Guidelines for their Applicability to Manufactured Nanomaterials Report* [ENV/JM/MONO(2009)21], 2009.

17. *OECD, Guidance on Sample Preparation and Dosimetry for the Safety Testing of Manufactured Nanomaterials*, 2012.

18. *OECD, Recommendation of the Council on the Safety Testing and Assessment of Manufactured Nanomaterials*, 2013.

19. P. Mulvaney, *Langmuir*, 1996, 12, 788-800.

20. E. Hutter and J. H. Fendler, *Advanced Materials*, 2004, 16, 1685-1706.

21. C. F. Phelps, *Biochemical Education*, 1977, 5, 22-22.

22. C. Cascio, D. Gilliland, F. Rossi, L. Calzolai and C. Contado, *Analytical Chemistry*, 2014, 86, 12143-12151.

23. R.Capomaccio, I. Ojea Jimenez, P. Colpo, D. Gilliland, G. Ceccone, F.Rossi and L. Calzolai. *Determination of the structure and morphology of gold nanoparticle–HSA protein complexes ,* Nanoscale, 2015, 7, 17653 DOI: 10.1039/C5NR05147A

24. J. Turkevich, P. C. Stevenson and J. Hillier, *Discussions of the Faraday Society*, 1951, 11, 55-75.

25. W. Haiss, N. T. K. Thanh, J. Aveyard and D. G. Fernig, *Analytical Chemistry*, 2007, 79, 4215-4221.

26. K. D. Hartlen, A. P. Athanasopoulos and V. Kitaev, *Langmuir*, 2008, 24, 1714-1720.

List of abbreviations and definitions

Agglomerate*	ISO/TS 80004-2:201 A collection of weakly bound particles or aggregates or mixtures of the two where the resulting external surface area is similar to the sum of the surface areas of the individual components
Aggregate**	ISO/TS 80004-2:201 A particle comprising strongly bonded or fused particles where the resulting external surface area may be significantly smaller than the sum of calculated surface areas of the individual components
CCM	Cell culture media
Cit	Citrate stabilised
CS	Calf Serum
CLS	Centrifugal Liquid Sedimentation
DLS	Dynamic Light Scattering
FBS	Foetal Bovine Serum
HS	Horse Serum
ICP-MS	Inductively Coupled Plasma mass Spectrometry
JRC	Joint Research Centre
NM	Nanomaterial
NMs	Nanomaterials
NP	Nanoparticle
OECD	Organisation for Economic Co-operation and Development
PVP	Polyvinylpyrrolidone
TEM	Transmission Electron Microscope
UV-Vis	UV-Visible
WPMN	Working Party of Manufactured Nanomaterials
Z-average	Zeta-average

(*/**) Use of terms agglomerate and aggregate

In this work no specific studies were conducted to distinguish between agglomerates and aggregates as defined above. In the absence of this information the term agglomerate will generally be used to refer to all collections of bound single particles, aggregates or mixtures of both irrespective of the effective bonding strength.

List of figures

List of tables

GETTING IN TOUCH WITH THE EU

In person

All over the European Union there are hundreds of Europe Direct information centres. You can find the address of the centre nearest you at: http://europea.eu/contact

On the phone or by email

Europe Direct is a service that answers your questions about the European Union. You can contact this service:

- by freephone: 00 800 6 7 8 9 10 11 (certain operators may charge for these calls),

- at the following standard number: +32 22999696, or

- by electronic mail via: http://europa.eu/contact

FINDING INFORMATION ABOUT THE EU

Online

Information about the European Union in all the official languages of the EU is available on the Europa website at: http://europa.eu

EU publications
You can download or order free and priced EU publications from EU Bookshop at: http://bookshop.europa.eu. Multiple copies of free publications may be obtained by contacting Europe Direct or your local information centre (see http://europa.eu/contact).

KJ-NA-29054-EN-N

JRC Mission

As the science and knowledge service of the European Commission, the Joint Research Centre's mission is to support EU policies with independent evidence throughout the whole policy cycle.

EU Science Hub
ec.europa.eu/jrc

@EU_ScienceHub

EU Science Hub - Joint Research Centre

Joint Research Centre

EU Science Hub

Publications Office

doi:10.2760/818663

ISBN 978-92-79-77705-9